A *CCR2-V64I* polymorphism affects stability of CCR2A isoform

Emi E. Nakayama, Yuetsu Tanaka,[a] Yoshiyuki Nagai,[b] Aikichi Iwamoto[c] and Tatsuo Shioda

Objective: A valine to isoleucine substitution at position 64 of CCR2 (*CCR2-64I*) is associated with a delay in progression to AIDS in HIV-1-infected individuals. The aim of the present study is to elucidate the molecular mechanism underlying the effect of this allele.

Design: We analysed the effect of the 64I substitution on levels of expression of CCR2A and CCR2B, two CCR2 isoforms produced by alternative splicing.

Methods: Sendai virus vector was used to express CCR2 molecules.

Results: While CCR2B trafficked well to the cell surface, CCR2A, which differs from CCR2B only by the sequence of its C-terminal cytoplasmic tail, was detected predominantly in the cytoplasm. The level of expression of CCR2A-64I was significantly higher than that of CCR2A without the substitution. On the other hand, the 64I substitution did not affect levels of CCR2B expression. Pulse–chase experiments revealed that the 64I substitution increased the half-life of CCR2A in cells. When co-expressed with CCR5, CCR2A-64I interfered more severely with cell surface expression of CCR5 than did wild-type CCR2A. Furthermore, immunoprecipitation experiments showed that CCR2A co-precipitated with an immature form of CCR5.

Conclusion: These results suggest that CCR2A binds to CCR5 in the cytoplasm and down-modulates its surface expression. We propose that the increased ability of CCR2A-64I to down-modulate CCR5 expression might be a possible cause of a delay in HIV-1 disease progression in patients with this allele.

AIDS 2004, **18**:729–738

Keywords: polymorphism, CCR2-64I, CCR2A, CCR5, stability

Introduction

The chemokine receptor CCR2B has been regarded as a minor HIV-1 coreceptor because only a small number of HIV-1 strains has been shown to use CCR2B as an entry coreceptor [1–3]. Nevertheless, a polymorphism in the CCR2 gene, *CCR2-64I*, has been reported to be associated with delayed disease progression in HIV-1 infected individuals in several Caucasian cohorts [4–8]. This polymorphism, a G-to-A transition at position 190, changes CCR2B codon 64 from valine to isoleucine, introducing a conservative amino acid change into the first transmembrane domain. It was unclear why a single amino acid substitution in a minor coreceptor could affect HIV-1 disease progression, as there was no difference in HIV-1 co-receptor activity between the variant CCR2B-64I and CCR2B without the 64I substitution (CCR2B-64V) [9,10]. Furthermore, these studies also excluded the possibility that CCR2B-64I exerts a dominant-negative effect on the expression and activity of CCR5.

From the Research Institute for Microbial diseases, Osaka University, Osaka, the [a]University of the Ryukyus, Okinawa, [b]Toyama Institute of Health, Toyama, and the [c]Institute of Medical Science, University of Tokyo, Tokyo, Japan.

Correspondence to T. Shioda, Department of Viral Infections, Research Institute for Microbial Diseases, Osaka University, 3-1 Yamada-oka, Suita-shi, Osaka 565-0871, Japan.

Received: 5 May 2003; revised: 27 September 2003; accepted: 15 October 2003.

DOI: 10.1097/01.aids.0000111407.02002.15

ISSN 0269-9370 © 2004 Lippincott Williams & Wilkins

It is possible that the *CCR2* polymorphism may be linked to other polymorphisms in genes that influence AIDS progression. The *CCR2* gene is located approximately 15 kb from the 5′ end of the *CCR5* gene, and the *CCR2-641* allele is indeed linked to a certain *CCR5* promoter haplotype [11]. However, experiments using promoter–reporter fusion constructs showed that the *CCR5* promoter haplotype, which is in a strong linkage disequilibrium with *CCR2-641*, did not affect transcriptional activity of the *CCR5* promoter [10]. Thus, the mechanism underlying the protective effect of *CCR2-641* against AIDS progression still remained to be elucidated.

Two alternatively spliced CCR2 isoforms, CCR2A and CCR2B, were reported to be present in freshly isolated human monocyte, THP-1, and MonoMac 6 leukaemia cell lines [12,13]. An open reading frame encoded in the chromosome corresponds to CCR2B, while alternatively spliced transcripts produce CCR2A. The two CCR2 isoforms differ only in their C-terminal cytoplasmic tails (Fig. 1). Therefore, an individual carrying the *CCR2-641* allele also produces CCR2A molecules with isoleucine at position 64. Although the cytoplasmic tail spans less than one-fifth of the entire CCR2 molecule, this difference caused a drastic alteration in their localization in cells [13]. While CCR2B trafficked well to the cell surface, CCR2A was detected predominantly in the cytoplasm. A progressive truncation study of the C-terminal cytoplasmic tail indicated that a cytoplasmic retention signal(s) was located in the C-terminal cytoplasmic tail [13]. Nevertheless, CCR2A molecules that successfully trafficked to the cell surface could respond to the stimulation of monocyte chemoattractant protein (MCP)-1 in a similar fashion to CCR2B [14].

As none of the previous studies investigated the effect

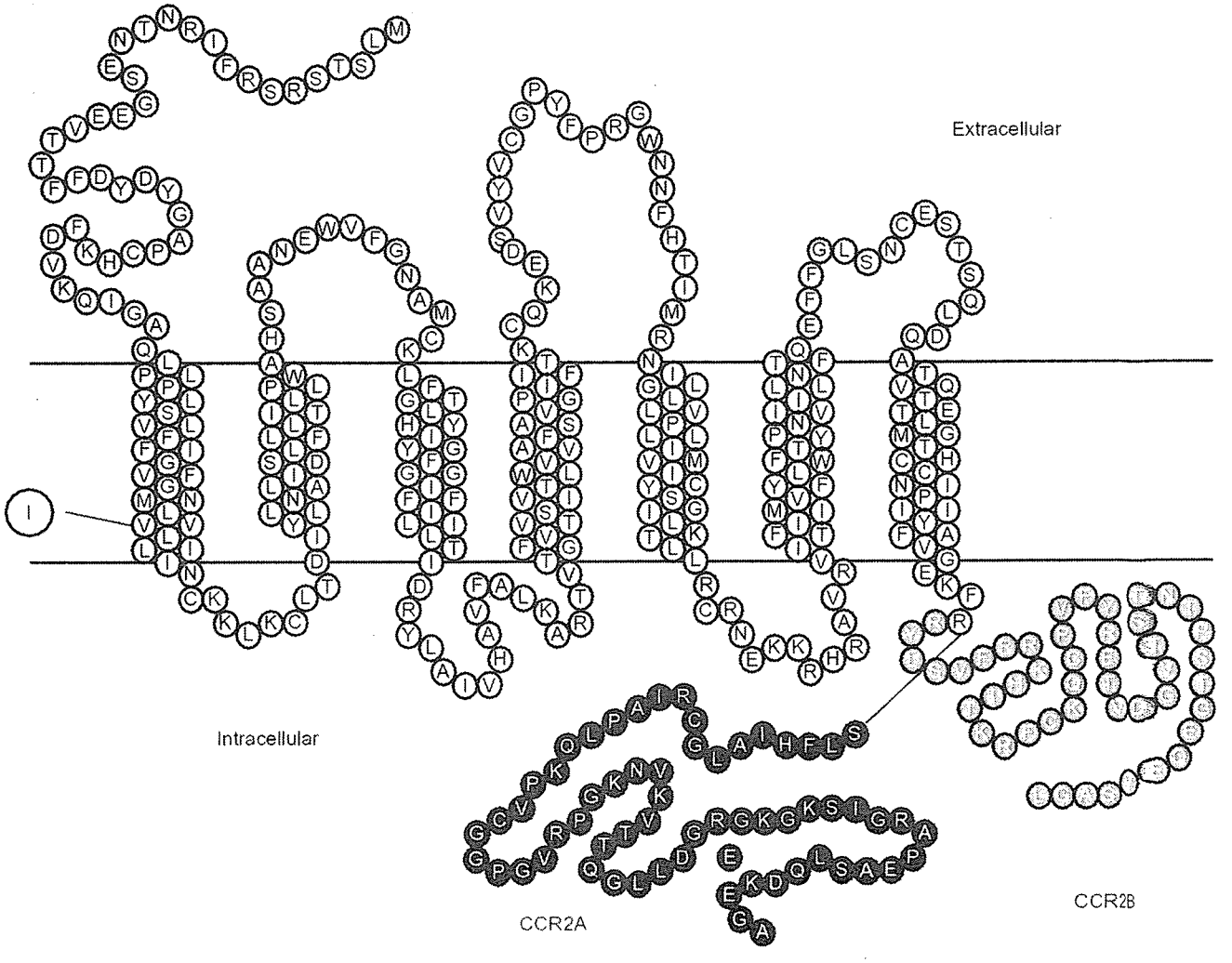

Fig. 1. The structure of the CCR2A and CCR2B molecules. Outlined letters in grey circles denote amino acid residues present in CCR2B. Outlined letters in black circles denote amino acid residues present in CCR2A. A letter I in a large circle denotes a substitution at position 64.

of the 64I substitution on CCR2A molecules, we generated recombinant Sendai viruses (SeV) expressing either CCR2A-64V or CCR2A-64I. Here we show that the 64I substitution indeed affected the stability of CCR2A molecules in cells, and increased the ability of CCR2A to down-modulate the major HIV-1 co-receptor, CCR5.

Materials and methods

Generation of recombinant SeV

THP-1 cells were shown to possess both *CCR2-64V* and *CCR2-64I* alleles by using a standard genotyping method [15]. Therefore, CCR2A-64V, CCR2A-64I, CCR2B-64V, and CCR2B-64I cDNA were obtained by reverse transcription (RT)-PCR from mRNA extracted from THP-1 cells and then inserted to the *Not*I site of pSeV18+b(+). The entire coding regions in the resultant plasmids were verified for sequence authenticity as well as for the presence or absence of the 64I substitution. For generating CCR2A-64V and CCR2A-64I cDNA carrying a c-myc-tag (EQKLI SEEDL) at their C-termini, cloned CCR2A-64V and CCR2A-64I cDNA served as templates for PCR amplification using a primer containing a nucleotide sequence corresponding the c-myc-tag fused with the C-terminal portion of CCR2A. Recombinant SeV carrying CCR2A-64V, CCR2A-64I, CCR2B-64V, CCR2B-64I, or C-myc-tagged versions of CCR2A-64V and CCR2A-64I were recovered according to a previously described method [16]. The wild-type Z strain of SeV served as a control in all the experiments.

Generation of a recombinant vaccinia virus

For generating CCR5 cDNA carrying a HA tag (YPYDVPDYAA) at its C terminus, cloned CCR5 cDNA served as a template for PCR amplification by using a primer containing a haemagglutinin (HA) tag sequence fused with the C-terminal portion of CCR5. The resultant PCR products were then inserted into pNZ68K2-Not. The entire coding region of CCR5-HA was verified for sequence authenticity. A recombinant vaccinia virus (Vac) was recovered from the resultant plasmid according to previously described procedures [17].

Flow cytometric analysis

CV1 monkey kidney cells, U937 monocytic cells and Jurkat T cells were infected with recombinant SeV expressing CCR2A-64V, CCR2A-64I, CCR2B-64V, or CCR2B-64I. Five to 18 h after infection, cells were incubated with MAB150, a mouse monoclonal antibody (MAb) against CCR2 (R & D Systems, Minneapolis, Minnesota, USA). Antibodies bound to cells were detected using fluorescein-5-isothiocyanate (FITC)-conjugated goat antibody directed against mouse IgG (Cappel, Aurora, Ohio, USA). CV1 or H9 cells infected with SeV expressing CCR2A-64V, CCR2A-64I, CCR2B-64V, or CCR2B-64I were superinfected with a recombinant Vac expressing CCR5, CXCR4, or CD4 at 9 h after SeV infection. After incubation for 5 h at 37°C, cells were stained for CCR5 using T227 rat MAb against CCR5 [17] followed by FITC-conjugated goat anti-rat IgG; for CXCR4 using 12G5 mouse MAb (R & D systems) followed by FITC-conjugated goat anti-mouse IgG; or for CD4 using FITC-conjugated anti-human CD4, Leu3a (Becton Dickinson, San Jose, California, USA), and analysed by FACScan (Becton Dickinson).

Immunofluorescence microscopy

CV1 cells expressing CCR2A or CCR2B were fixed and permeabilized before being incubated with MAB150 antibody as described previously [17]. Bound antibodies were then detected using FITC-conjugated goat antibody against mouse IgG. Indirect immunofluorescence was visualized using a Lasersharp2000 Confocal Microscope System (Bio-Rad, Hercules, California, USA). Anti-Calnexin (Stressgen, San Diego, California, USA) or anti-Giantin (CRPinc, Berkeley, California, USA) rabbit polyclonal antibody was used with Cy5-conjugated goat antibody against rabbit IgG (Amersham Pharmacia Biotech, Piscataway, New Jersey, USA).

Chemotaxis assay

Chemotaxis assays were performed according to previously described methods [18]. Briefly, MCP-1 (PeproTech, Rockey Hill, New Jersey, USA) diluted at an indicated concentration of chemotaxis buffer (RPMI 1640 with 0.25% human serum albumin) was added to the bottom chamber of a 5-μm pore polycarbonate Transwell culture insert (Costar; Corning, New York, USA). Jurkat cells were infected with a SeV expressing CCR2A-64V or CCR2A-64I and incubated at 37°C for 4 h. Cells were then washed with RPMI1640 and re-suspended in chemotaxis buffer and added to the upper chamber of the insert. Transmigrated cells in 4 h at 37°C were counted using a FACScan.

Pulse-chase analyses of CCR2A and CCR5

CV1 or U937 cells were infected with a SeV expressing CCR2A-64V-myc or CCR2A-64I-myc. Nine hours after infection, cells were labelled with 500 kbq/ml of EXPRE^{35}S^{35}S[^{35}S] protein labelling mix (> 37 Tbq/mmol; PerkinElmer (Boston, Massachusetts, USA) in amino acid-free medium for 30 min. For CCR5 analysis, cells were infected with a recombinant Vac expressing CCR5-HA, incubated at 37°C for 5 h and then labelled. Cells were then washed, fed with fresh medium and incubated for 0, 15, 30, 60, or 120 min at 37°C, chilled on ice, and lysed in lysis buffer (50 mM Tris-HCl pH7.5, 150 mM NaCl, 1% Nonidet P40, 0.5% sodium deoxycholate). CCR2A

and CCR5 proteins in the lysates were precipitated with anti-myc mouse MAb (9B11; Cell Signaling, Beverly, Massachusetts, USA) and anti-HA high affinity rat MAb (Roche, Indianapolis, Indiana, USA), respectively, using a Protein G Immunoprecipitation Kit (Roche). Precipitated materials were subjected to SDS–PAGE on a 4–12% NuPAGE Bis–Tris gel (Invitrogen, Groningen, Netherlands), and the amount of radiolabel incorporated was visualized on a BAS Imager (Fujix, Kanagawa, Japan).

Gene reporter fusion assay

A recombinant Vac-based gene activation assay using a β-galactosidase gene as a reporter was performed as described previously [19]. Briefly, mouse fibroblast L cells were transfected with β-galactosidase reporter plasmid pGINT7β-gal and infected with a recombinant Vac expressing gp160 of an R5 HIV-1 strain SF162. At the same time, CV1 cells were infected with SeV expressing CCR2A-64V or CCR2A-64I and incubated at 37°C for 9 h. Cells were then superinfected with recombinant Vacs expressing T7 RNA polymerase, human CD4, and CCR5, detached by trypsinization, and cultured at 37°C for 5 h. Then, L and CV-1cells were mixed, incubated for 3 h, and β-galactosidase activities in the cell lysate were measured by using chlorophenol red-β-D-galactopyranoside as substrate.

HIV-1 productive infection

MT4 cells (4×10^5) were infected with SeV expressing CCR2A-64V, CCR2A-64I or parental Z strain of SeV at a multiplicity of infection (MOI) of 40 plaque forming unit (PFU)/cell mixed with SeV expressing CCR5 at an MOI of 10 PFU/cell and incubated at 37°C for 5 h. Cells were then superinfected with 60 ng p24 of an R5 HIV-1 strain SF162. The culture supernatants were collected periodically and p24 levels were measured.

Immunoprecipitation and western blot analysis

CV1 cells were infected with SeV expressing CCR2A-64V-myc or CCR2A-64I-myc, and incubated at 37°C for 9 h. Cells were then superinfected with a Vac expressing CCR5-HA and incubated at 37°C for 5 h and then lysed. CCR2A-64V-myc, CCR2A-64I-myc or CCR5-HA proteins were immunoprecipitated, and subjected to SDS–PAGE as described above. Proteins were then electrophoretically transferred to a PVDF membrane (Immobilon; Millipore, Bedford, Massachusetts, USA). Blots were blocked and probed with the antibodies overnight at 4°C and then incubated with peroxidase-conjugated anti-mouse (Kirkegaard & Perry Laboratories, Gaithersbug, Maryland, USA) or anti-rat IgG (American Qualex, San Clemente, California, USA) and developed using the Immun-Star HRP chemiluminescent kit (Bio-Rad).

Results

Expression of CCR2A and CCR2B

We generated a recombinant SeV expressing either CCR2A-64V or CCR2B-64V. Confocal microscopic observations (Fig. 2a) and flow cytometric analyses (Fig. 2b) confirmed the different subcellular localization of these two CCR2 isoforms. In CCR2B-64V expressing CV1 cells, fluorescent signals of CCR2 were observed mainly on the cell surface. In contrast, CCR2A-64V was localized predominantly to the cytoplasm, although a small portion of CCR2A was observed on the cell surface. In the cytoplasm, signals of an endoplasmic reticulum marker calnexin were only partially co-localized with CCR2A signals (Fig. 2a, left), whereas the majority of signals for the Golgi marker giantin overlapped with those of CCR2A (Fig. 2a, right). These results suggested that most CCR2A molecules were retained in the Golgi.

To assess the effect of the 64I substitution on CCR2A expression, we generated a recombinant SeV expressing CCR2A-64I and compared levels of expression of CCR2A-64I with those of CCR2A-64V. As shown in Fig. 2b, CCR2A-64I showed slightly but significantly higher levels of expression than CCR2A-64V in various cell types, despite the same promoter being used. The mean fluorescence intensity (MFI) of CCR2A-64I and CCR2A-64V was 274 and 140 in CV1, 133 and 40 in U937 monocystic cells, and 29 and 21 in Jurkat T cells. The difference was greater in U937 cells than in Jurkat cells. The difference was also observed at 5, 12, and 18 h after infection of recombinant SeVs (Fig. 2c). Exactly the same result was obtained when recombinant SeV expressing C-myc-tagged versions of CCR2A-64V (CCR2A-64V-myc) and CCR2A-64I (CCR2A-64I-myc) were used (Fig. 2c). In contrast, we failed to detect any difference in the levels of expression between CCR2B-64V and CCR2B-64I (MFI 2698 and 2663, respectively; Fig. 2b), as had been described in the previous reports [9,10]. Northern blot analyses confirmed that there was no difference in the amount of CCR2 mRNA among cells expressing CCR2A-64V, CCR2A-64I, CCR2A-64V-myc, CCR2A-64I-myc, CCR2B-64V and CCR2B-64I (data not shown). These data clearly indicate that the substitution of valine to isoleucine affects levels of cell surface expression of CCR2A, but not of CCR2B.

Chemokine receptor activity of recombinant CCR2A-64V and CCR2A-64I

To determine whether or not CCR2A molecules expressed by a recombinant SeV fully retained chemokine receptor activity, we performed a chemotaxis assay. As shown in Fig. 2d, both cells expressing CCR2A-64V and CCR2A-64I migrate toward MCP-1. However, cells expressing CCR2A-64I migrated

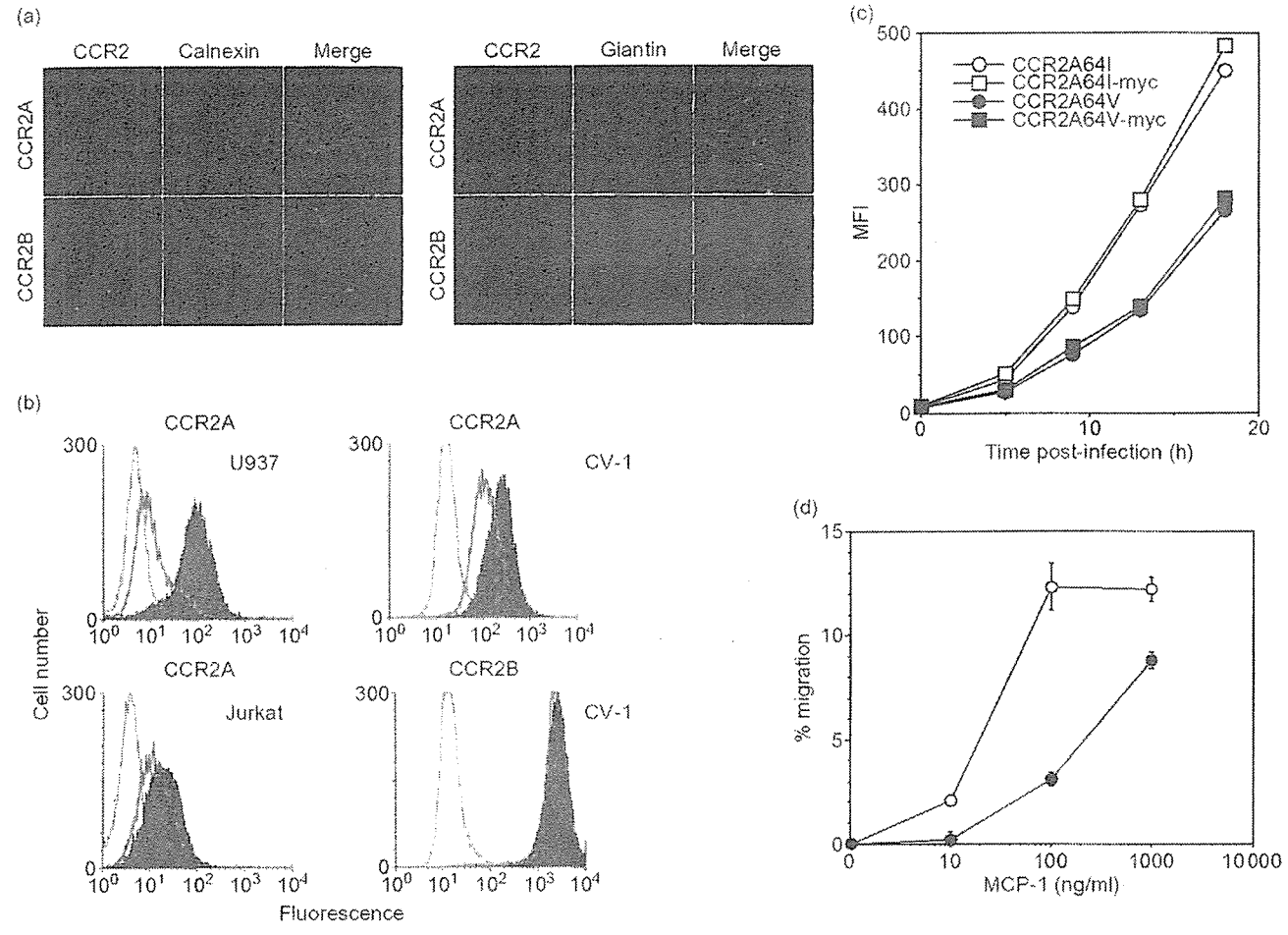

Fig. 2. (a) Subcellular distribution of CCR2A-64V and CCR2B-64V in CV1 cells. SeV vector (SeV) was used to express the CCR2A-64V and CCR2B-64V molecules. Cells were fixed and permeabilized before staining with MAB150 anti-CCR2 mouse MAb followed by FITC-labelled anti-mouse IgG. Cells were then re-stained with anti-calnexin or anti-giantin rabbit polyclonal antibody followed by Cy5-labelled anti-rabbit IgG, and analysed by confocal laser microscopy. (b) Surface expression of CCR2A-64V (green) and CCR2A-64I (red) in U937, CV1 or Jurkat cells. Cells infected with the parental Z strain served as a negative control (black). In lower right panel, green and red indicates CCR2B-64V and CCR2B-64I, respectively. (c) The cell surface expression of CCR2A-64I (open circles), CCR2A-64I-myc (open squares), CCR2A-64V (filled circles), and CCR2A-64V-myc (filled squares) at 5, 9, 12 and 18 h after infection by SeV. MFI indicates mean fluorescence intensity of each sample. (d) Chemokine receptor activity of recombinant CCR2A-64V and CCR2A-64I. Jurkat cells infected with SeV expressing CCR2A-64V (closed circles) or CCR2A-64I (open circles) migrated in response to increasing concentration of MCP-1. Data points are means of triplicate determination with standard deviations.

more efficiently than those expressing CCR2A-64V. These results are in good agreement with the observation that expression of CCR2A-64I is higher than that of CCR2A-64V.

CCR2A-64I is more stable than CCR2A-64V

Differential levels of expression between CCR2A-64V and CCR2A-64I prompted us to compare the rate of degradation of those proteins in pulse–chase experiments. For this purpose, we used recombinant SeV expressing CCR2A-64V-myc or CCR2A-64I-myc. Comparison of immunoprecipitated materials from ^{35}S-labelled CV1 cells expressing CCR2A-64V-myc and CCR2A-64I-myc showed that almost identical levels of CCR2A-64V-myc and CCR2A-64I-myc proteins were synthesized during the 30-min labelling period (t = 0) (Fig. 3a). However, CCR2A-64V-myc proteins appeared to degrade more rapidly than CCR2A-64I-myc proteins. The half-life of CCR2A-64I-myc was approximately 90 min, whereas that of CCR2A-64V-myc was approximately 50 min in CV1 cells (Fig. 3b). More prominent results were obtained when we used U937 cells, as the half-life of CCR2A-64I-myc was approximately 60 min, whereas that of CCR2A-64V-myc was approximately 18 min in U937 cells. This finding is in a good agreement with the observation

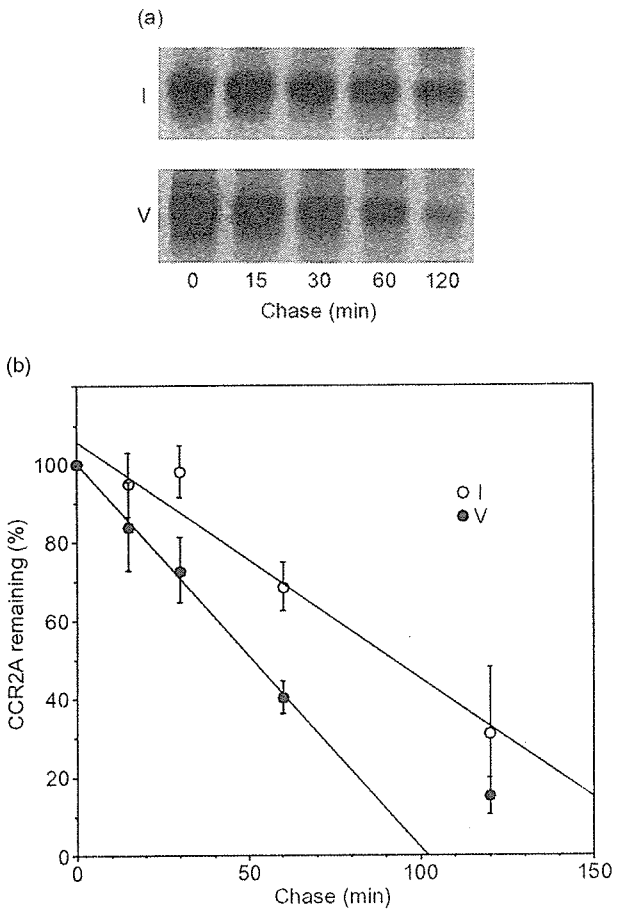

Fig. 3. CCR2A-64I is more stable than CCR2A-64V. CV1 cells were infected with SeV expressing CCR2A-64V-myc and CCR2A-64I-myc for 9 h. Cells were labelled for 30 min and then harvested following the chase time indicated. (a) Representative gels of pulse-chase analysis. (b) Phosphorlmager analysis of the gels shown in (a). Open and closed circles denote cells infected with SeV expressing CCR2A-64V-myc and CCR2A-64I-myc, respectively. Data points are means of four independent experiments with standard deviations.

that the difference in cell surface expression levels between CCR2A-64V and CCR2A-64I was greater in U937 cells than in CV-1 cells (Fig. 2b). These results indicate that higher cell surface expression of CCR2A-64I was due to increased stability of CCR2A-64I. On the other hand, we failed to detect any significant difference in the half-life between CCR2B-64V and CCR2B-64I (data not shown).

CCR5 but not CXCR4 expression was more severely blocked by co-expression of CCR2A-64I than by co-expression of CCR2A-64V

To determine whether or not CCR2A has a dominant-negative effect on the expression of major HIV-1 receptor molecules, we first inoculated SeV expressing CCR2A-64V or CCR2A-64I in CV1 cells and incubated the cells for 9 h at 37°C. The cells were then superinfected with recombinant Vac expressing CCR5, CXCR4, or CD4. Five hours after Vac infection, surface expression of CCR5, CXCR4, or CD4 were examined by flow cytometry. As shown in Fig. 4a, the CCR5 MFI of cells co-infected with parental Z strain of SeV was 391, while that of the cells co-infected with SeV expressing CCR2A-64V was 297, indicating that co-expression of CCR2A-64V significantly reduced levels of CCR5 expression on the cell surface. This dominant-negative effect on CCR5 expression was more prominent when SeV expressing CCR2A-64I were used (MFI, 145) than SeV expressing CCR2A-64V were used. The same results were obtained when we used recombinant SeV expressing CCR2A-64V-myc and CCR2A-64I-myc (MFI, 300 and 179, respectively). Similar results were obtained when CV1 cells were inoculated with Vac expressing CCR5 5 h after infection by SeV expressing CCR2A, as the CCR5 MFI on cells co-infected with Z, SeV expressing CCR2A-64V, and Sev expressing CCR2A-64I, was 299, 205, and 160, respectively. Furthermore, the dominant-negative effect of CCR2A on CCR5 expression was also observed when T cell line H9 was used. The CCR5 MFI on H9 cells co-infected with Z, SeV expressing CCR2A-64V, and SeV expressing CCR2A-64I was 263, 230 and 195, respectively. In contrast, the cell surface expression of CXCR4, another major co-receptor, as well as that of CD4, the main receptor of HIV-1, were not affected by CCR2A-64V or CCR2A-64I (Fig. 4a). In contrast with CCR2A, neither CCR2B-64V nor CCR2B-64I affected the surface expression of CCR5 (Fig. 4b).

HIV-1 coreceptor activity of CCR5 was more dramatically reduced by co-expression of CCR2A-64I than by co-expression of CCR2A-64V

To assess the effect of CCR2A-64I on HIV-1 infection, we examined the ability of cells expressing both CCR2A and CCR5 molecules to support CD4-dependent cell fusion mediated by an HIV-1 envelope protein of the R5 strain SF162. For this purpose, we prepared CV1 cells expressing both CCR5 and CCR2A as described in Fig. 4a, and mixed those cells with mouse L cells expressing HIV-1 envelope protein. As shown in Fig. 5a, the envelope-mediated cell fusion activity of CCR5 was more dramatically reduced by co-expression of CCR2A-64I than by that of CCR2A-64V.

We also inoculated a live SF162 strain of HIV-1 into CD4 positive MT4 cells expressing both CCR5 and CCR2A. As shown in Fig. 5b, MT4 cells expressing CCR5 and CCR2A-64V supported SF162 replication better than those expressing CCR5 and CCR2A-64I.

Co-immunoprecipitation of CCR2A and CCR5

Many seven-transmembrane receptors, including che-

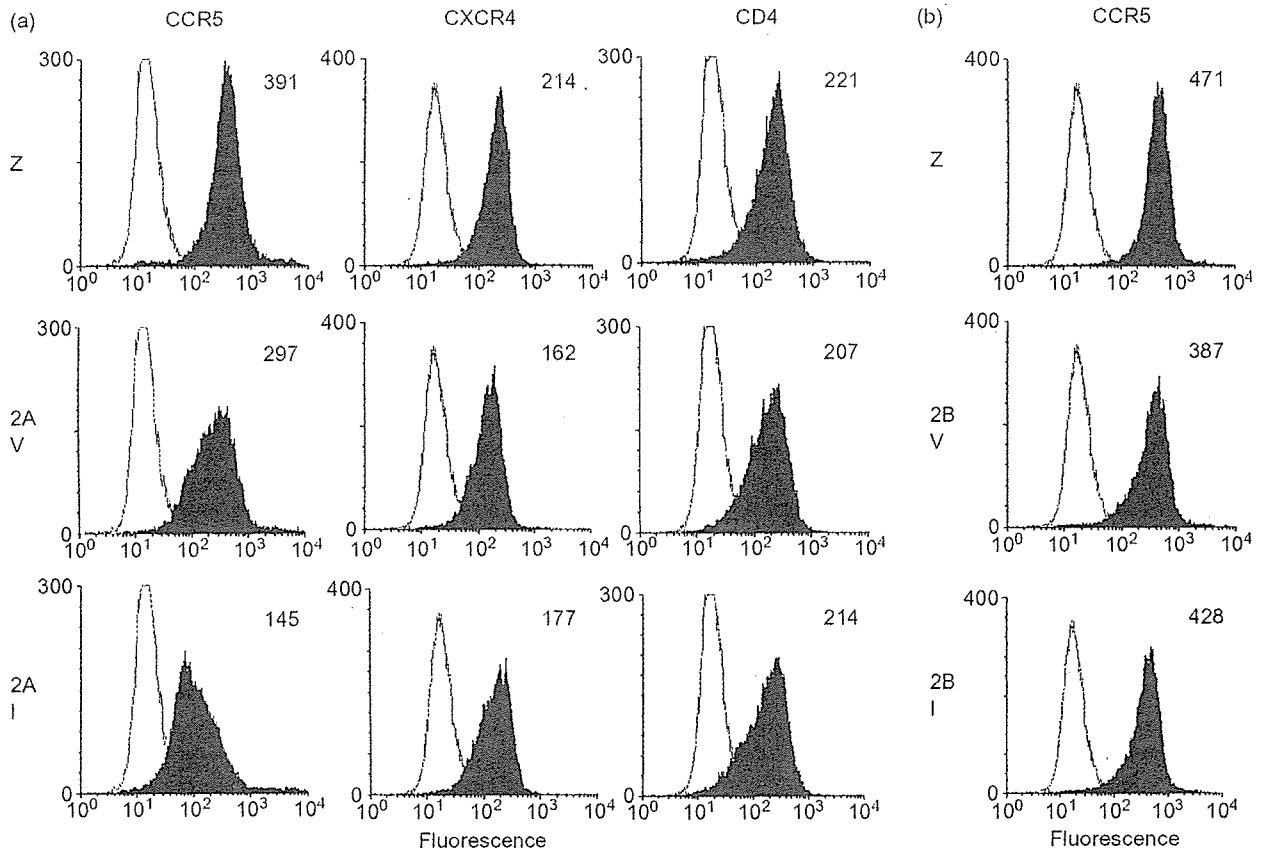

Fig. 4. (a) Effect of CCR2A-64V and CCR2A-64I on HIV-1 corecepter expression. Vac vectors were used to express CCR5, CXCR4 and CD4 in the CV1 cells inoculated with SeV expressing CCR2A-64V or CCR2A-64I. Z denotes the wild-type SeV. Five hours after infection, cells were stained with MAb against CCR5, CXCR4, or CD4. Flow cytometry was used to determine surface expression levels. The number in each panel indicates mean fluorescence intensity. (b) Effect of CCR2B-64V and CCR2B-64I on CCR5 expression.

mokine receptors, have been reported to form homo-oligomers. CCR2A is highly homologous to CCR5 (68% at the amino acid level), and formation of heterodimers between CCR2B and CCR5 was reported previously [20]. The dominant-negative effect of CCR2A on CCR5 expression shown in Figs 4a, 5a and 5b raised the possibility of heterodimer formation between CCR2A and CCR5. To test this hypothesis, we used SeV expressing CCR2A-64V-myc or CCR2A-64I-myc, and Vac expressing HA-tagged version of CCR5 (CCR5-HA). Anti-myc and anti-HA immunoprecipitates from cell lysates were developed in Western blots by using anti-HA or anti-myc antibodies. As expected, CCR5-HA was detected by anti-HA antibody in anti-myc-derived immunoprecipitates from CCR5-HA and CCR2A-64V-myc co-expressed cell lysates as well as from CCR5-HA and CCR2A-64I-myc co-expressed cell lysates. At the same time, CCR2A-64V-myc and CCR2A-64I-myc were detected by anti-myc antibody in anti-HA-derived immunoprecipitates of CCR5-HA and CCR2A-64V-myc co-expressed cell lysates and in that of CCR5-HA and CCR2A-64I-myc co-expressed cell lysates (Fig. 5c). These results clearly indicate that CCR2A formed heterodimers with CCR5.

In CCR5-HA expressing cells, we consistently observed two types of CCR5-HA molecules with different electrophoretic mobility. When we used anti-HA antibody to precipitate CCR5-HA directly, most of the CCR5-HA molecules migrated at approximately 38 kDa. In contrast, most of the CCR5-HA molecules that co-precipitated with CCR2A-64V-myc or CCR2A-64I-myc migrated at 37 kDa. We speculated that the CCR5-HA of 38 kDa represented authentic CCR5 molecules and that of 37 kDa represented immature forms of CCR5. To verify the maturation process of CCR5, we labelled the cells infected with Vac expressing CCR5-HA by [^{35}S]-methionine for 30 min and harvested those cells following chase periods ranging from 15 to 60 min. As shown in Fig. 5d, the 37-kDa CCR5-HA could be detected only after the labelling period (0 min). This result suggests that CCR2A binds to premature forms of CCR5 and

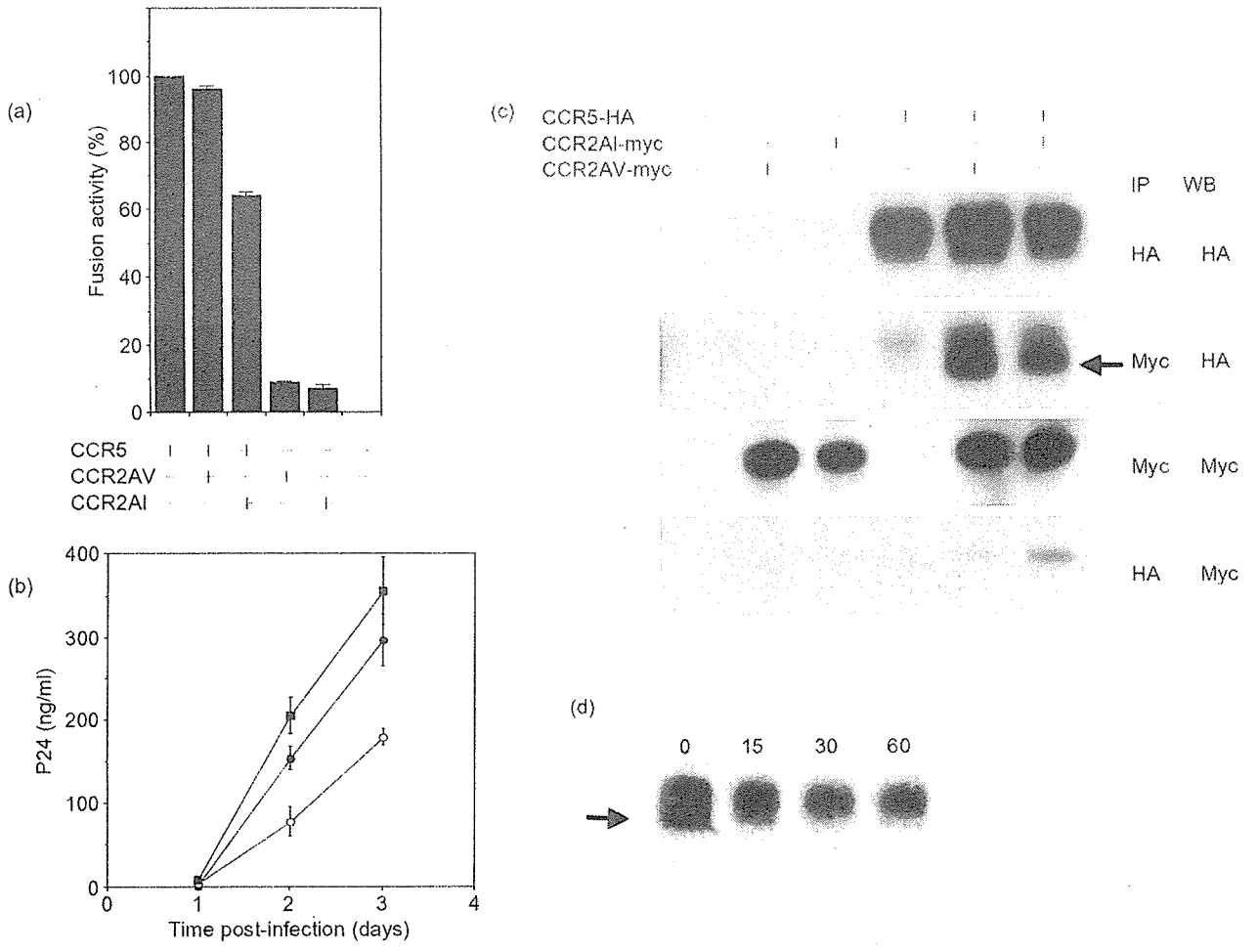

Fig. 5. (a) Coreceptor activity of CCR5 in CCR2A-64V or CCR2A-64I co-expressed cells. SeV vector was used to express CCR2A-64V or CCR2A-64I, and Vac vector was used to express CCR5 as described in Fig. 4. HIV-1 coreceptor activity of each sample was measured using the method described in Materials and methods. The wild-type Vac WR strain was used as a CCR5-negative control, and the wild-type SeV Z strain was used as the CCR2A-negative control. (b) MT4 cells were co-infected with SeV expressing CCR5 and SeV expressing CCR2A-64V (filled circles), CCR2A-64I (open circles), or parental Z strain (filled squares). Five hours after infection, cells were inoculated with an HIV-1 strain SF162. (c) Co-immunopresipitation of CCR2A and CCR5. Recombinant Vac expressing CCR5-HA or parental WR strain (-) was superinfected in CV1 cells infected with SeVs expressing CCR2A-64V-myc, CCR2A-64I-myc, or the parental Z strain (-). Immunoprecipitation and Western blot analysis were performed by using anti-HA or anti-myc antibody. An arrow indicates 37-kDa CCR5-HA molecules. (d) Pulse chase analysis of CCR5 molecules. A recombinant Vac expressing CCR5-HA was inoculated into CV1 cells. An arrow indicates 37-kDa CCR5-HA molecules.

interferes with the maturation process of CCR5 molecules in cytoplasm.

Discussion

Many independent cohort studies have affirmed the AIDS-delaying effects of the *CCR2-64I* allele [4–8], but the molecular mechanism of this protective effect had not yet been elucidated. In the present study, we demonstrated that a valine to isoleucine substitution at position 64 increased stability of CCR2A but not of CCR2B molecules in cells. When co-expressed with the major HIV-1 co-receptor CCR5, CCR2A-64I more severely interfered with cell surface expression as well as HIV-1 co-receptor activity of CCR5 than CCR2A-64V. Furthermore, CCR2A was shown to co-precipitate with immature form of CCR5. These results suggest that CCR2A binds to CCR5 in the cytoplasm and dominantly interferes with CCR5 maturation and surface expression. On the other hand, the 64I substitution did not affect the level of CCR2B expression, being consistent with results published previously [9,10]. We speculate that increased ability of CCR2A-64I to down modulate CCR5 expression

might be a possible cause of delay in HIV-1 disease progression in patients with this allele. Alternatively, it is also possible that immune cell trafficking and/or signalling might be affected by CCR2A stabilization, leading to a delay in HIV-1 diseases.

Previously, Mellado *et al.* reported that CXCR4 could dimerize with CCR2B-64I variants but not with wild-type CCR2B-64V upon stimulation with SDF-1 and MCP-1. Based on this finding, they proposed that this ability of CCR2B-64I to heterodimerize with CXCR4 may cause a delay in AIDS progression [20]. However, several independent cohort studies have shown that the effects of the *CCR2-64I* allele were more pronounced in earlier stages of disease than in latter stages [5,8,21]. In a Dutch cohort, delay in HIV-1 disease progression was more pronounced before the emergence of X4 variants and was not observed after the emergence of X4 variants in individuals with the CCR2-64I allele [6]. Therefore, it is unlikely that CCR2B-64I/CXCR4 heterodimerization is the main cause of delay in AIDS progression in individuals with CCR2-64I.

Previous studies exploring the oligomerization of chemokine receptors also yielded controversial results. Rodrigues-Frade *et al.* reported that CCR2B forms homodimers upon stimulation by MCP-1 [22]. Other studies, however, have shown that CCR5 [23,24] and CXCR4 [25] can form homodimers without any stimulation by their ligands. Although we did not test whether or not stimulation with MCP-1 and/or RANTES increases hetero-oligomer formation between CCR2A and CCR5, our present results support the latter model that chemokine receptors may form oligomers without stimulation by their ligands.

In addition to AIDS pathogenesis, the CCR2-64I allele was reported to be associated with lower risks of coronary artery calcification [26] and acute rejection in renal transplantation [27]. Our present results shed light onto possible mechanisms of the association of this allele with such diverse human phenotypes. It is now widely accepted that monocyte attachment to cardiovascular wall is the first event implicated in atherogenesis of coronary arteries [28,29]. Since monocytes are known to express both CCR2A and CCR2B [13], an increased stability of CCR2A resulting from the 64I substitution may interfere with the function of CCR2B in monocytes, leading to decreased monocyte invasion to cardiovascular walls. With respect to acute rejection in renal transplantation, CCR5 is known to play an important role in both rejection of renal transplantation [30] and experimental graft-versus-host disease models [31]. Therefore, it is possible that an increased ability of CCR2A-64I to interfere with CCR5 expression can cause a decreased frequency of acute rejection after renal transplantation in recipients with this allele.

Previous studies have failed to show a statistically significant difference in levels of CCR5 expression on stimulated or non-stimulated peripheral blood mononuclear cells between CCR2-64I homozygotes and CCR2-64V homozygotes [9,10,32], although a slight reduction was noted in CCR2-64I homozygotes. In fact, we also failed to observe a statistically significant reduction of CCR5 levels on peripheral CD4 cells of homozygotes of CCR2-64I (data not shown). CCR2 is reported to be expressed on monocytes/macrophages [33], basophils [34,35], B cells [36], NK cells [37], dendritic cells [38,39], and a limited population of T cells [40]. Although we observed very few CCR2 cells in peripheral blood mononuclear cells, Bartoli *et al.* reported that numerous mononuclear cells in tonsil expressed CCR2A [41]. It may be possible that specific cell types expressing both CCR2A and CCR5 in tonsil or lymph nodes play an important role in AIDS pathogenesis and are responsible for the delay in HIV-1 diseases observed in patients with CCR2-64I.

Acknowledgements

pGFT7 beta-gal was kindly supplied by E. Berger. We thank D. Chao for critical discussion and S. Bando for technical assistance.

Sponsorship: Supported by grants from the Human Science Foundation, the Ministry of Education, Culture, Sports, Science, and Technology, and the Ministry of Health, Labour and Welfare, Japan.

References

1. Doranz BJ, Rucker J, Yi Y, Smyth RJ, Samson M, Peiper SC, *et al.* **A dual-tropic primary HIV-1 isolate that uses fusin and the beta-chemokine receptors CKR-5, CKR-3, and CKR-2b as fusion cofactors.** *Cell* 1996, 85:1149–1158.
2. Rucker J, Edinger AL, Sharron M, Samson M, Lee B, Berson JF, *et al.* **Utilization of chemokine receptors, orphan receptors, and herpesvirus- encoded receptors by diverse human and simian immunodeficiency viruses.** *J Virol* 1997, 71:8999–9007.
3. Penton-Rol G, Cota M, Polentarutti N, Luini W, Bernasconi S, Borsatti A, *et al.* **Up-regulation of CCR2 chemokine receptor expression and increased susceptibility to the multitropic HIV strain 89.6 in monocytes exposed to glucocorticoid hormones.** *J Immunol* 1999, 163:3524–3529.
4. Smith MW, Dean M, Carrington M, Winkler C, Huttley GA, Lomb DA, *et al.* **Contrasting genetic influence of CCR2 and CCR5 variants on HIV-1 infection and disease progression. Hemophilia Growth and Development Study (HGDS), Multicenter AIDS Cohort Study (MACS), Multicenter Hemophilia Cohort Study (MHCS), San Francisco City Cohort (SFCC), ALIVE Study.** *Science* 1997, 277:959–965.
5. Kostrikis LG, Huang Y, Moore JP, Wolinsky SM, Zhang L, Guo Y, *et al.* **A chemokine receptor CCR2 allele delays HIV-1 disease progression and is associated with a CCR5 promoter mutation.** *Nat Med* 1998, 4:350–353.
6. van Rij RP, de Roda Husman AM, Brouwer M, Goudsmit J, Coutinho RA, Schuitemaker H. **Role of CCR2 genotype in the clinical course of syncytium-inducing (SI) or non-SI human immunodeficiency virus type 1 infection and in the time to**

conversion to SI virus variants. *J Infect Dis* 1998, **178**: 1806–1811.
7. Ioannidis JP, Rosenberg PS, Goedert JJ, Ashton LJ, Benfield TL, Buchbinder SP, *et al.* **Effects of CCR5-Delta32, CCR2-64I, and SDF-1 3'A alleles on HIV-1 disease progression: An international meta-analysis of individual- patient data.** *Ann Intern Med* 2001, **135**:782–795.
8. Mulherin SA, O'Brien TR, Ioannidis JP, Goedert JJ, Buchbinder SP, Coutinho RA, *et al.* **Effects of CCR5-Delta32 and CCR2-64I alleles on HIV-1 disease progression: the protection varies with duration of infection.** *AIDS* 2003, **17**:377–387.
9. Lee B, Doranz BJ, Rana S, Yi Y, Mellado M, Frade JM, *et al.* **Influence of the CCR2-V64I polymorphism on human immunodeficiency virus type 1 coreceptor activity and on chemokine receptor function of CCR2b, CCR3, CCR5, and CXCR4.** *J Virol* 1998, **72**:7450–7458.
10. Mariani R, Wong S, Mulder LC, Wilkinson DA, Reinhart AL, LaRosa G, *et al.* **CCR2-64I polymorphism is not associated with altered CCR5 expression or coreceptor function.** *J Virol* 1999, **73**:2450–2459.
11. Mummidi S, Ahuja SS, Gonzalez E, Anderson SA, Santiago EN, Stephan KT, *et al.* **Genealogy of the CCR5 locus and chemokine system gene variants associated with altered rates of HIV-1 disease progression.** *Nat Med* 1998, **4**: 786–793.
12. Charo IF, Myers SJ, Herman A, Franci C, Connolly AJ, Coughlin SR. **Molecular cloning and functional expression of two monocyte chemoattractant protein 1 receptors reveals alternative splicing of the carboxyl-terminal tails.** *Proc Natl Acad Sci USA* 1994, **91**:2752–2756.
13. Wong LM, Myers SJ, Tsou CL, Gosling J, Arai H, Charo IF. **Organization and differential expression of the human monocyte chemoattractant protein 1 receptor gene. Evidence for the role of the carboxyl-terminal tail in receptor trafficking.** *J Biol Chem* 1997, **272**:1038–1045.
14. Sanders SK, Crean SM, Boxer PA, Kellner D, LaRosa GJ, Hunt SW, 3rd. **Functional differences between monocyte chemotactic protein-1 receptor A and monocyte chemotactic protein-1 receptor B expressed in a Jurkat T cell.** *J Immunol* 2000, **165**:4877–4883.
15. Louisirirotchanakul S, Liu H, Roongpisuthipong A, Nakayama EE, Takebe Y, Shioda T, *et al.* **Genetic analysis of HIV-1 discordant couples in Thailand: association of CCR2 64I homozygosity with HIV-1-negative status.** *J Acquir Immune Defic Syndr* 2002, **29**:314–315.
16. Kato A, Sakai Y, Shioda T, Kondo T, Nakanishi M, Nagai Y. **Initiation of Sendai virus multiplication from transfected cDNA or RNA with negative or positive sense.** *Genes Cells* 1996, **1**:569–579.
17. Shioda T, Nakayama EE, Tanaka Y, Xin X, Liu H, Kawana-Tachikawa A, *et al.* **Naturally occurring deletional mutation in the C-terminal cytoplasmic tail of CCR5 affects surface trafficking of CCR5.** *J Virol* 2001, **75**:3462–3468.
18. Shioda T, Kato H, Ohnishi Y, Tashiro K, Ikegawa M, Nakayama EE, *et al.* **Anti-HIV-1 and chemotactic activities of human stromal cell-derived factor 1alpha (SDF-1alpha) and SDF-1beta are abolished by CD26/dipeptidyl peptidase IV-mediated cleavage.** *Proc Natl Acad Sci USA* 1998, **95**:6331–6336.
19. Nakayama EE, Shioda T, Tatsumi M, Xin X, Yu D, Ohgimoto S, *et al.* **Importance of the N-glycan in the V3 loop of HIV-1 envelope protein for CXCR-4- but not CCR-5-dependent fusion.** *FEBS Lett* 1998, **426**:367–372.
20. Mellado M, Rodriguez-Frade JM, Vila-Coro AJ, de Ana AM, Martinez AC. **Chemokine control of HIV-1 infection.** *Nature* 1999, **400**:723–724.
21. Michael NL, Louie LG, Rohrbaugh AL, Schultz KA, Dayhoff DE, Wang CE, *et al.* **The role of CCR5 and CCR2 polymorphisms in HIV-1 transmission and disease progression.** *Nat Med* 1997, **3**:1160–1162.
22. Rodriguez-Frade JM, Vila-Coro AJ, de Ana AM, Albar JP, Martinez AC, Mellado M. **The chemokine monocyte chemoattractant protein-1 induces functional responses through dimerization of its receptor CCR2.** *Proc Natl Acad Sci USA* 1999, **96**: 3628–3633.
23. Benkirane M, Jin DY, Chun RF, Koup RA, Jeang KT. **Mechanism of transdominant inhibition of CCR5-mediated HIV-1 infection by ccr5delta32.** *J Biol Chem* 1997, **272**:30603–30606.
24. Issafras H, Angers S, Bulenger S, Blanpain C, Parmentier M, Labbe-Jullie C, *et al.* **Constitutive agonist-independent CCR5 oligomerization and antibody- mediated clustering occurring at physiological levels of receptors.** *J Biol Chem* 2002, **277**: 34666–34673.
25. Babcock GJ, Farzan M, Sodroski J. **Ligand-independent dimerization of CXCR4, a principal HIV-1 coreceptor.** *J Biol Chem* 2003, **278**:3378–3385.
26. Valdes AM, Wolfe ML, O'Brien EJ, Spurr NK, Gefter W, Rut. A, *et al.* **Val64Ile polymorphism in the C-C chemokine receptor 2 is associated with reduced coronary artery calcification.** *Arterioscler Thromb Vasc Biol* 2002, **22**:1924–1928.
27. Abdi R, Tran TB, Sahagun-Ruiz A, Murphy PM, Brenner BM, Milford EL, *et al.* **Chemokine receptor polymorphism and risk of acute rejection in human renal transplantation.** *J Am Soc Nephrol* 2002, **13**:754–758.
28. Ross R. **The pathogenesis of atherosclerosis: a perspective for the 1990s.** *Nature* 1993, **362**:801–809.
29. Hanke H, Lenz C, Finking G. **The discovery of the pathophysiological aspects of atherosclerosis–a review.** *Acta Chir Belg* 2001, **101**:162–169.
30. Segerer S, Cui Y, Eitner F, Goodpaster T, Hudkins KL, Mack M, *et al.* **Expression of chemokines and chemokine receptors during human renal transplant rejection.** *Am J Kidney Dis* 2001, **37**:518–531.
31. Murai M, Yoneyama H, Harada A, Yi Z, Vestergaard C, Guo B, *et al.* **Active participation of CCR5(+)CD8(+) T lymphocytes in the pathogenesis of liver injury in graft-versus-host disease.** *J Clin Invest* 1999,104:49-57.
32. Shieh B, Liau YF, Hsieh PS, Yan YP, Wang ST, Li C. **Influence of nucleotide polymorphisms in the CCR2 gene and the CCR5 promoter on the expression of cell surface CCR5 and CXCR4.** *Int Immunol* 2000, **12**:1311–1318.
33. Fantuzzi L, Borghi P, Ciolli V, Pavlakis G, Belardelli F, Gessani S. **Loss of CCR2 expression and functional response to monocyte chemotactic protein (MCP-1) during the differentiation of human monocytes: role of secreted MCP-1 in the regulation of the chemotactic response.** *Blood* 1999, **94**:875–883.
34. Ochensberger B, Tassera L, Bifrare D, Rihs S, Dahinden CA. **Regulation of cytokine expression and leukotriene formation in human basophils by growth factors, chemokines and chemotactic agonists.** *Eur J Immunol* 1999, **29**:11–22.
35. Iikura M, Miyamasu M, Yamaguchi M, Kawasaki H, Matsushima K, Kitaura M, *et al.* **Chemokine receptors in human basophils: inducible expression of functional CXCR4.** *J Leukoc Biol* 2001, **70**:113–120.
36. Frade JM, Mellado M, del Real G, Gutierrez-Ramos JC, Lind P, Martinez AC. **Characterization of the CCR2 chemokine receptor: functional CCR2 receptor expression in B cells.** *J Immunol* 1997, **159**:5576–5584.
37. Polentarutti N, Allavena P, Bianchi G, Giardina G, Basile A, Sozzani S, *et al.* **IL-2-regulated expression of the monocyte chemotactic protein-1 receptor (CCR2) in human NK cells: characterization of a predominant 3.4-kilobase transcript containing CCR2B and CCR2A sequences.** *J Immunol* 1997, **158**:2689–2694.
38. Sallusto F, Schaerli P, Loetscher P, Schaniel C, Lenig D, Mackay CR, *et al.* **Rapid and coordinated switch in chemokine receptor expression during dendritic cell maturation.** *Eur J Immunol* 1998, **28**:2760–2769.
39. Vanbervliet B, Homey B, Durand I, Massacrier C, Ait-Yahia S, de Bouteiller O, *et al.* **Sequential involvement of CCR2 and CCR6 ligands for immature dendritic cell recruitment: possible role at inflamed epithelial surfaces.** *Eur J Immunol* 2002, **32**:231–242.
40. Rabin RL, Park MK, Liao F, Swofford R, Stephany D, Farber JM. **Chemokine receptor responses on T cells are achieved through regulation of both receptor expression and signaling.** *J Immunol* 1999, **162**:3840–3850.
41. Bartoli C, Civatte M, Pellissier JF, Figarella-Branger D. **CCR2A and CCR2B, the two isoforms of the monocyte chemoattractant protein-1 receptor are up-regulated and expressed by different cell subsets in idiopathic inflammatory myopathies.** *Acta Neuropathol (Berl)* 2001, **102**:385–392.

Cross-Talk between Activated Human NK Cells and CD4$^+$ T Cells via OX40-OX40 Ligand Interactions[1]

Alessandra Zingoni,*† Thierry Sornasse,[2]‡ Benjamin G. Cocks,‡ Yuetsu Tanaka,§ Angela Santoni,† and Lewis L. Lanier[3]*

It is important to understand which molecules are relevant for linking innate and adaptive immune cells. In this study, we show that OX40 ligand is selectively induced on IL-2, IL-12, or IL-15-activated human NK cells following stimulation through NKG2D, the low affinity receptor for IgG (CD16) or killer cell Ig-like receptor 2DS2. CD16-activated NK cells costimulate TCR-induced proliferation, and IFN-γ produced by autologous CD4$^+$ T cells and this process is dependent upon expression of OX40 ligand and B7 by the activated NK cells. These findings suggest a novel and unexpected link between the natural and specific immune responses, providing direct evidence for cross-talk between human CD4$^+$ T cells and NK receptor-activated NK cells. *The Journal of Immunology,* **2004, 173: 3716–3724.**

For an effective T cell response at least two signals are needed: the first is delivered by TCR interaction with MHC and peptide, and the second involves ligation of costimulatory receptors. Costimulation can involve augmenting cell proliferation, cell survival, and/or the production of cytokines. Many receptors have now been described to be costimulatory, including receptors of the Ig superfamily, such as CD28 and ICOS, and receptors of the TNF superfamily. Interactions between TNF ligands and TNFR family members, including for example OX40 ligand (OX40L) and OX40, have been implicated in T cell costimulation (1). Expression of OX40L is inducible and has been reported on several hemopoietic cell types, including dendritic cells (2), B cells (3), T cells, and microglial cells, as well as on vascular endothelial cells (4). OX40L expression is induced on APCs several days after activation by CD40L-CD40 interactions or by inflammatory stimuli (1, 2). Recently, high levels of OX40L have been shown to be expressed on a new type of CD3$^-$CD4$^+$ accessory cell, located in B cell follicles, capable of promoting survival of Th2 cells through OX40-OX40L interactions (5). OX40 is expressed predominantly by activated CD4$^+$ T cells (6). OX40$^+$ cells are found in the T cell zones of lymphoid organs following priming with Ag (3), and also have been detected in situ in several inflammatory states, including experimental autoimmune encephalomyelitis, rheumatoid arthritis, chronic synovitis, graft-vs-host disease, and on tumor-infiltrating lymphocytes (6–9). Ligation of OX40 on CD4$^+$ T cells by agonist reagents can increase clonal expansion and cytokine production (10), enhance memory T cell development (11), and augment anti-tumor immunity (12). OX40 has also been shown to play an important role in the stimulation of anti-viral CD4$^+$ T cell responses in vivo (13).

NK cells are lymphocytes that provide innate immunity against tumors and virus-infected cells. A balance of signals received from multiple activating and inhibitory receptors regulates their effector functions (14). These receptors allow NK cells to rapidly survey their environment for danger. When an imbalance in signaling favors activation, secretion of cytokines and/or release of cytotoxic granules occurs (14). In humans, NKG2D is one of the activating receptors that is expressed on NK cells, γδ T cells, and CD8αβ T cells (15). NKG2D recognizes as ligands UL16-binding protein 1 (ULBP1), ULBP2, ULBP3, ULBP4, and the MHC class I chain-related molecules, MICA and MICB (15, 16). These NKG2D ligands are generally absent or expressed at low levels on most healthy cells, but can be induced by viral (17) and bacterial infections (18, 19). In addition, they are frequently up-regulated in many epithelial tumors (20) and in "stressed" cells (21).

Several studies have focused on the ability of NK cells to regulate adaptive immune responses through the production of Th1-type cytokines early during infection (22) or through the activation of dendritic cells (23). In addition, by establishing cocultures of NK- and Ag-activated T cells, it has been shown that human NK cells can be induced to secrete IFN-γ in response to IL-2 produced by activated T cells (24). In contrast, much less has been reported about the physical interactions that may take place between NK cells and adaptive immune cells, in particular CD4$^+$ T cells.

In this study, we show that OX40L can be induced on human NK cells by stimulation through their activating NK receptors. In addition, we present direct evidence for cross-talk between CD4$^+$ T cells and NK cells in which OX40-OX40L and CD28-B7 interactions contribute to T cell proliferation and IFN-γ production in response to TCR-induced activation.

Materials and Methods

Reagents, cytokines, Abs, and flow cytometry

Human rIL-12 and IL-15 were purchased from BioSource International (Camarillo, CA). The National Cancer Institute Biological Resources

*Department of Microbiology and Immunology and the Cancer Research Institute, University of California, San Francisco, CA 94143; †Department of Experimental Medicine and Pathology, University of Rome "La Sapienza", Rome, Italy; ‡Incyte Corporation, Palo Alto, CA 94304; and §Department of Immunology, Graduate School and Faculty of Medicine, University of the Ryukyus, Okinawa, Japan

Received for publication May 18, 2004. Accepted for publication June 18, 2004.

The costs of publication of this article were defrayed in part by the payment of page charges. This article must therefore be hereby marked *advertisement* in accordance with 18 U.S.C. Section 1734 solely to indicate this fact.

[1] L.L.L. is an American Cancer Society Research Professor, and A.Z. was a recipient of an American-Italian Cancer Foundation Fellowship and of a research contract with the University of Rome "La Sapienza". These studies were supported by National Institutes of Health Grant CA89294 and a grant from Associazione Italiana per la Ricerca sul Cancro to A.S.

[2] Current address: Protein Design Labs, Inc., Pre-Clinical and Clinical Development Sciences, 34801 Campus Drive, Fremont, CA 94555.

[3] Address correspondence and reprint requests to Dr. Lewis L. Lanier, Department of Microbiology and Immunology and the Cancer Research Institute, University of California, 513 Parnassus Avenue, San Francisco, CA 94143. E-mail address: lanier@itsa.ucsf.edu

[4] Abbreviations used in this paper: OX40L, OX40 ligand; cIg, control Ig; SEB, staphylococcal enterotoxin B; ULBP, UL16-binding protein; KIR, killer cell Ig-like receptor.

0022-1767/04/$02.00

Branch Preclinical Repository (Frederick, MD) generously provided human rIL-2. Staphylococcal enterotoxin B (SEB) and PHA were purchased from Sigma-Aldrich (St. Louis, MO). The following mouse anti-human mAbs were used: anti-killer cell Ig-like receptor (KIR)2DS2 (DX27), neutralizing anti-CD80 (L307), and anti-CD86 (IT2.2) (BD Pharmingen, San Diego, CA), FITC-conjugated anti-CD80 (BU63; Caltag Laboratories, Burlingame, CA), FITC-conjugated anti-CD86 (MEM-233; Caltag Laboratories), anti-CD8α (Leu2a; BD Pharmingen), anti-CD4 (Leu3a; BD Pharmingen), anti-HLA-DR (BD Pharmingen), anti-NKG2D (clone 149810; R&D Systems, Minneapolis, MN), anti-CD56 (DX32), neutralizing anti-OX40L (5A8) (2, 4), anti-CD16 (B73.1) (kindly provided by Dr. G. Trinchieri, Schering-Plough, Dardilly, France), and anti-CD3 (OKT3; American Tissue Culture Collection, Manassas, VA). PE-conjugated goat anti-mouse IgG was purchased from Jackson ImmunoResearch Laboratories (West Grove, PA), FITC-conjugated anti-mouse IgG was purchased from Zymed Laboratories (South San Francisco, CA), and goat anti-mouse IgG $F(ab')_2$ was from Cappel Laboratories (ICN Biomedicals, Opera, Milan, Italy). Cells were analyzed by using a FACSCalibur (BD Biosciences, San Jose, CA) or a small desktop Guava Personal Cytometer with Guava ViaCount and Guava Express software (Burlingame, CA). Viable lymphocyte populations were gated based on forward and side scatters and by propidium iodide staining.

Cell lines, plasmids, and transfectants

The NKL cell line, generously provided by Dr. Mike Robertson (25), was cultured in RPMI 1640 medium supplemented with 10% FCS, 2 mM L-glutamine, 100 U/ml penicillin, 100 μg/ml streptomycin, and 200 U/ml human rIL-2. Cells were cultured at a density of 5×10^5/ml in a 37°C incubator with 5% CO_2. For all experiments, cells were grown at a density of 1×10^6/ml in medium containing IL-2. Generation of NKL stably expressing KIR2DS2 was described previously (26). Because mouse Ba/F3 pro-B cells are IL-3 dependent for their proliferation, the Ba/F3 cells used in these experiments were transfected with an expression plasmid containing the mouse cDNA IL-3 to provide for autocrine growth (kindly provided by Dr. S. Tangye, Centenary Institute, Sydney, Australia). MICA transfectants were established by retroviral transduction using the pMX-pie vector (27, 28) containing a MICA*0019 cDNA.

Preparation of NK cells and T cells

Small resting $CD4^+$ T lymphocytes were purified as follows: PBMC were isolated by lymphoprep density gradient centrifugation, monocytes and B cells were removed by adherence to nylon wool, then cells were labeled with anti-CD8, anti-CD56, anti-HLA-DR, and anti-CD19 mAbs, and these cells were mixed with magnetic beads coated with goat anti-mouse IgG (Dynal Biotech, Oslo, Norway). Thereafter, $CD8^+$, $CD19^+$, $HLA\text{-}DR^+$, and $CD56^+$ cells were removed by magnetic cell sorting. The remaining cells were >98% $CD4^+CD3^+$, as assessed by immunofluorescence and flow cytometric analysis. Polyclonal NK cell cultures were obtained by coculturing nylon nonadherent PBMC with irradiated (3000 rad) RPMI 8866 B cells for 9–10 days at 37°C in a humidified 5% CO_2 atmosphere, as previously described (29). NK cell cultures were >90% $CD16^+CD56^+CD3^-$, as assessed by immunofluorescence and flow cytometric analysis. Contaminating T cells were depleted by magnetic cell sorting, yielding a final NK population >98% $CD16^+CD56^+CD3^-$.

Stimulation of the cells, RNA preparation, microarrays, and data analysis

Twenty-four-well culture plates were coated with goat anti-mouse IgG (5 μg/ml, in carbonate buffer, pH 9.6) at 37°C for 4 h. Wells were washed three times with PBS and primary Abs were added to each well at 10 μg/ml, or amounts indicated in the figures, and incubated overnight at 4°C in PBS. When in combination with anti-NKG2D mAb, anti-KIR2DS2 mAb was used at 0.5 μg/ml. NKL cells were plated at 2×10^6/ml in each well in 500 μl of medium. $Poly(A)^+$ RNA was isolated using an mRNA isolation kit (Qiagen, Valencia, CA) according to the manufacturer's protocol. Gene expression modulation between unstimulated and stimulated NKL cells was evaluated by using Incyte standard procedures (Palo Alto, CA), as described elsewhere (30). Briefly, $poly(A)^+$ RNA were labeled with Cy3 or Cy5 fluorescent labeling dyes using reverse transcription, followed by hybridization onto a Human Drug Target 1 microarray (Incyte) (31, 32). This microarray contained a total of 9129 elements representing a total of 8481 unique gene clusters whose identity was confirmed by stringent PCR verification during manufacturing. The Cy3/Cy5 ratio for each element was considered valid if the signal to background ratios for both dyes exceeded 2.5, and if the signal of either dye exceeded 250 fluorescence units. A total of 6125 elements returned valid Cy3/Cy5 ratios for all 20 hybridizations (10 treatments hybridized in duplicates). Elements were further selected based on a minimum Cy3/Cy5 ratio of 2-fold in either direction in at least one experimental condition, yielding 406 elements of interest. These elements of interest were then clustered using an agglomerative clustering algorithm (Ward's method, JMP; SAS Institute, Cary, NC). All data are expressed in $\log_2$, where negative values denote gene up-regulation (Cy3 < Cy5) and reciprocally, positive values represent gene down-regulation (Cy3 > Cy5).

Cytokine and proliferation assays

Homogeneous populations of cultured human primary NK cells were activated for 72 h with IL-2 (100 U/ml) and stimulated with anti-CD16 plate-bound mAb for 18 h. In some experiments, NK cells were preactivated with IL-15 (10 ng/ml) or IL-12 (10 U/ml). Dead cells were removed by Ficoll-gradient centrifugation. NK cells were fixed with 1% paraformaldehyde (in PBS, pH 7.4) for 7 min at room temperature. Different numbers of NK cells were plated with 1×10^5 highly purified autologous $CD4^+$ T cells, and cultured for 5 days in the presence of soluble anti-CD3 mAb (5 μg/ml) or SEB (0.5–25 ng/ml) or PHA (50 ng/ml). Blocking Ab against OX40L and/or CD80 and CD86 was added on day 0 at 5 μg/ml. Wells were pulsed with 0.5 μCi of [^{3}H]thymidine for the final 18 h of culture, and incorporated radioactivity was measured in a scintillation counter. Data are represented as the mean of cpm ± SD (triplicates). In some experiments, supernatants were collected at day 3 or 5, and the amount of IL-4 and IFN-γ was quantified by specific ELISA kits (BioSource International).

Results

Microarray analysis shows up-regulation of OX40L following triggering of NK-activating receptors on a human NK cell line

Microarray analysis was used to characterize genes up-regulated by the stimulation of NKG2D alone or in combination with the DAP12-associated KIR2DS2-activating receptor. As a model, we used a human NK cell line, NKL, which constitutively expresses the DAP10-associated NKG2D receptor (33), and was transfected with KIR2DS2 (26). Because NKG2D alone is an insufficient stimulus for the transcription-dependent production of IFN-γ (26, 34), this cell system is particularly useful because it provided the opportunity to evaluate the efficacy of NKG2D costimulation using as a read out the amplification of KIR2DS2-induced IFN-γ (Ref. 26 and data not shown). $Poly(A)^+$ mRNA from resting and stimulated NKL cells was extracted, and cDNA was prepared for the comprehensive analysis of gene transcription by using microarray technology. A Human Drug Target 1 Incyte microarray containing a total of 9128 elements was used. Analysis of data was performed using a hierarchical clustering algorithm to group genes with similar expression patterns across all the samples. We focused our attention on a group of seven genes that were amplified significantly following the simultaneous cross-linking of KIR2DS2 and NKG2D receptors (Table I). These genes included three chemokines (i.e., lymphotactin, MIP-1β, and CCL18), granzymes B and H, the platelet-activating receptor homologue (a seven transmembrane receptor of unknown function), and the TNF member OX40L (CD134L). Among this group of genes, OX40L mRNA was the only one that was up-regulated by NKG2D cross-linking alone (Table I). Previously, OX40L expression has been implicated predominantly in the function of APCs, such as activated monocytes, dendritic cells, and B cells. Thus, this unexpected finding prompted us to investigate the role of OX40L in human NK cell function.

Results from the microarray experiment were confirmed by showing that cross-linking KIR2DS2, NKG2D, and KIR2DS2 plus NKG2D indeed enhanced transcription of OX40L in NKL cells, as determined by quantitative RT-PCR analysis (data not shown). More importantly, KIR2DS2- and NKG2D-induced activation resulted in an increased expression of OX40L on the cell surface of NKL cells, as determined by using a specific anti-OX40L mAb

Table 1. *Microarray analysis of NKL cells stimulated through NKG2D and/or KIR2DS2*[a]

Gene Name	Accession Number	cIg	KIR2DS2	NKG2D	KIR2DS2 + NKG2D
Lymphotactin	AL031736	0.31	−0.85	0.48	−2.39
MIP-1β	AV758471	0.06	−1.03	−0.07	−2.14
Granzyme H	NM_004131	0.43	−0.58	0.96	−1.87
Granzyme B	M57888	0.12	−0.48	0.81	−1.74
PAR	NM_013308	0.32	−0.72	0.07	−1.63
OX40L	**BE349175**	**0.13**	**−0.68**	**−0.20**	**−1.26**
CCL18	NM_00298	0.48	−0.58	0.14	−1.42

[a] Differential expression ratios of control Ig (cIg)-treated NKL cells (Cy3) compared to anti-KIR2DS2 and/or anti-NKG2D-treated NKL cells (Cy5) expressed in $\log_2$. Negative values represent up-regulation of transcription compared with cIg-stimulated cells.

(Fig. 1*A*). Stimulation with high doses of anti-KIR mAb or anti-NKG2D mAb alone substantially up-regulated OX40L on the surface of NKL cells. In addition, anti-NKG2D mAb augmented up-regulation of OX40L on NKL cells stimulated with a suboptimal dose of anti-KIR mAb (Fig. 1*A*).

OX40 is expressed predominantly on activated $CD4^+$ T cells and prior studies have shown that interactions between OX40 on activated $CD4^+$ T cells and OX40L on APCs can augment T cell proliferation and cytokine production. Therefore, studies were performed to determine whether OX40L-bearing NK cells could costimulate $CD4^+$ T cell proliferation. NKL cells, which constitutively express OX40L (Fig. 1*A*), were cocultured with freshly isolated human $CD4^+$ T cells and were stimulated with anti-CD3 mAb or PHA. As shown in Fig. 1*B*, NKL indeed augmented $CD4^+$ T cell proliferation, and this activity was blocked, in part, in the presence of a neutralizing anti-OX40L mAb. These studies indicated that OX40L on NKL is functional and contributes to the proliferation of $CD4^+$ T cells. However, these studies were complicated by the necessity to use allogeneic $CD4^+$ T cells and also because NKL is a long-term NK cell line established from a patient with NK cell leukemia (25). Therefore, it was important to validate these findings using autologous NK cells and T cells from normal healthy individuals.

Both cytokines and NK receptor-mediated stimulation are required to induce OX40L on human peripheral blood NK cells

Freshly isolated, highly purified human peripheral blood NK cells do not express OX40L on the cell surface (data not shown), although a prior study had reported the presence of OX40L transcripts (35). Because the NKL cell line requires IL-2 for growth, we investigated whether OX40L could be induced on peripheral blood NK cells from healthy adults simply by culture in the presence of IL-2 or other cytokines known to stimulate NK cells, e.g., IL-12 and IL-15. As shown in Fig. 2*A*, culture of normal human peripheral blood NK cells in IL-2, IL-12, or IL-15 failed to induce OX40L. Therefore, based on the observation that OX40L was up-regulated in NKL cells stimulated through its activating receptors, we stimulated human polyclonal NK cells through CD16, an IgG FcR that signals via the ITAM-bearing FcεRIγ and CD3ζ adapter proteins. Whereas treatment with cytokines alone failed to induce OX40L, the majority (typically 60% or more) of normal NK cells stimulated by plate-bound anti-CD16 mAb together with IL-2, IL-12, and IL-15 expressed OX40L at high levels on the cell surface (Fig. 2*A*). Stimulation with anti-CD16 mAb in the absence of IL-2 (or IL-12 or IL-15) induced OX40L only on a small proportion of NK cells. A dose-dependent induction of OX40L was observed when NK cells were activated with anti-CD16 mAb in the presence of IL-2 (Fig. 2*B*). In contrast to OX40L, culture of peripheral blood NK cells in IL-2 only did induce expression of CD86 (Fig. 2*C*) and this was not enhanced by stimulation with anti-CD16 mAb (Fig. 2*D*). CD80, another ligand of the CD28 costimulatory receptor on T cells, was not induced by IL-2 (Fig. 2*C*), and there was only a very slight indication of CD80 induction when both IL-2 and anti-CD16 stimulation were combined (Fig. 2*D*).

Because studies using the NKL cell line indicated that stimulation through the NKG2D receptor up-regulated OX40L, we also investigated this using peripheral blood NK cells from healthy adults. Polyclonal populations of NK cells from healthy individuals were expanded in culture, preactivated with IL-2 and stimulated with a plate-bound mAb against NKG2D. Fig. 3*A* shows that NKG2D cross-linking induced OX40L on ~20% of the NK cells.

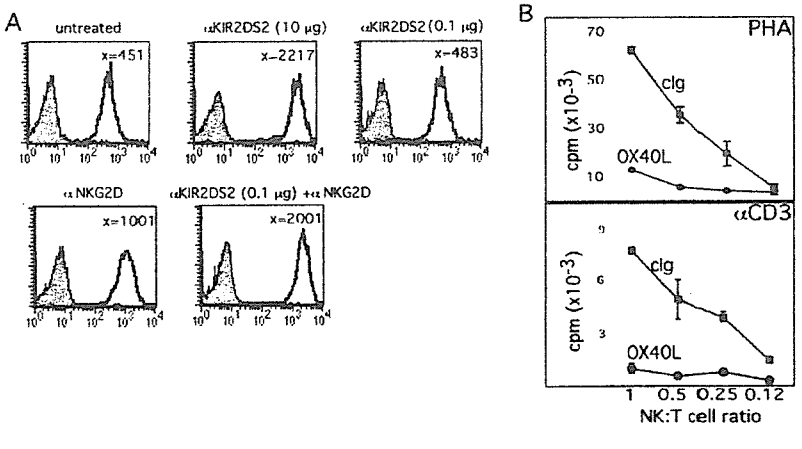

FIGURE 1. Up-regulation of OX40L on NKL by NK receptors and costimulation of $CD4^+$ T cell proliferation. *A*, NKL cells were stimulated with plate-bound mAb anti-NKG2D (10 μg/ml), anti-KIR2DS2 (10 μg/ml or 0.1 μg/ml), or both for 18 h. Cells were harvested and stained with PE-conjugated anti-OX40L mAb (open histograms) or with an isotype-matched cIg (filled histograms). *B*, Different amounts of paraformaldehyde-fixed NKL cells were cultured with 1×10^5 $CD4^+$ T cells in the presence of soluble anti-CD3 (5 μg/ml) or PHA (50 ng/ml). Neutralizing anti-OX40L mAb was added at day 0 and cocultures were harvested at day 5. Cultures were pulsed with 0.5 μCi of [^{3}H]thymidine for the final 18 h, and incorporated radioactivity was measured in a scintillation counter. A representative experiment of three is shown. Data are represented as the mean of cpm ± SD.

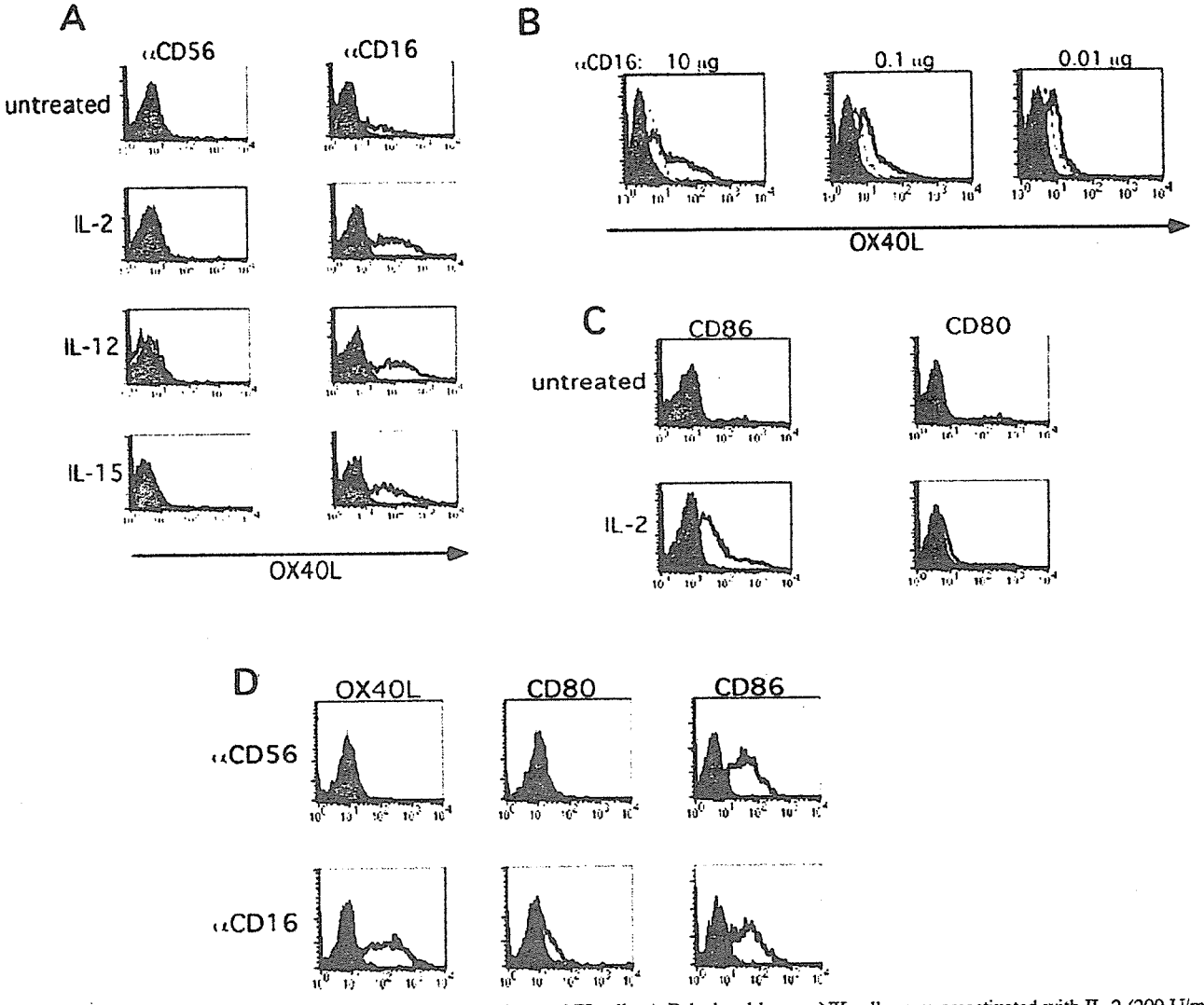

FIGURE 2. Induction of OX40L and B7 family members on human NK cells. *A*, Polyclonal human NK cells were preactivated with IL-2 (200 U/ml), IL-15 (10 ng/ml), or IL-12 (10 U/ml) for 48 h, and stimulated with plate-bound anti-CD16 mAb (saturating concentration). Plate-bound anti-CD56 mAb was used as a negative control. After 18 h of culture, cells were harvested and stained with PE-conjugated anti-OX40L mAb (thick line, open histograms) or with a cIg (filled histograms). *B*, IL-2-activated polyclonal NK cells were stimulated with different amounts (10 μg/ml, 0.1 μg/ml, and 0.01 μg/ml) of plate-bound anti-CD16 mAb (thick line). Plate-bound anti-CD56 mAb (dotted line) was used as a negative control for stimulation. Cells were harvested after 18 h and stained with FITC-conjugated anti-OX40L mAb (open histograms) or a cIg (filled histograms). A representative experiment of five is shown. *C*, Peripheral blood NK cells were cultured in the presence of IL-2 (200 U/ml) for 72 h and stained with FITC–conjugated anti-CD80 (thick lines, open histograms), FITC–conjugated anti-CD86 (thick lines, open histograms), or a cIg (filled histograms). *D*, IL-2-activated polyclonal NK cells were stimulated for 18 h with anti-CD16 or anti-CD56 (negative control) plate-bound mAbs. Cells were stained with PE-conjugated anti-OX40L mAb, FITC–conjugated anti-CD80 (thick lines, open histograms), FITC–conjugated anti-CD86 (thick lines, open histograms), or a cIg (filled histograms). In this experiment, CD86 was induced on these NK cells by coculture in IL-2, but was not further increased by stimulation with the anti-CD56 mAb used as a control.

As observed with anti-CD16 stimulation, induction of OX40L required both pretreatment with IL-2 and NKG2D activation because neither condition alone induced OX40L (data not shown). The ability of NKG2D stimulation to induce OX40L on NK cells was further validated by activation using stimulator cells bearing MICA, a physiological ligand of the NKG2D receptor. IL-2-preactivated peripheral blood NK cells were cocultured for 18 h with different ratios of the mouse pro-B cell line Ba/F3 or Ba/F3 cells stably expressing human MICA. As with anti-NKG2D mAb stimulation, OX40L was induced on ~20% of the IL-2-activated NK cells cocultured with $MICA^+$Ba/F3 cells, but not the untransfected Ba/F3 cells (Fig. 3*B*). Analysis of the kinetics of OX40L expression on human NK cells following stimulation with MICA-bearing cells showed that OX40L expression was transient; it was expressed rapidly after 5 h, peaked at 18 h, and then declined between 32 to 48 h poststimulation (Fig. 3*C*). These IL-2-activated NK cells were able to efficiently kill the $MICA^+$Ba/F3 cells, but not the untransfected Ba/F3 cells, demonstrating that the NKG2D receptor on the NK cells was specifically activated (data not shown).

Therefore, both by stimulation with anti-NKG2D mAb and by interaction with $MICA^+$Ba/F3 cells, we observed induction of OX40L on a subset comprising ~20% of IL-2-activated peripheral blood NK cells (Fig. 3). An examination of the phenotype of the NK cells stimulated by either anti-NKG2D or $MICA^+$Ba/F3 cells revealed that OX40L was induced on both the $CD56^{bright}CD16^{-/low}$ and on the $CD56^{int}CD16^{high}$ peripheral blood NK cell subsets, although within these subsets a relatively higher fraction of the $CD56^{bright}CD16^{-/low}$ NK cells expressed OX40L (our unpublished observation). Therefore, the subset of peripheral blood NK cells presenting OX40L after NKG2D stimulation was not

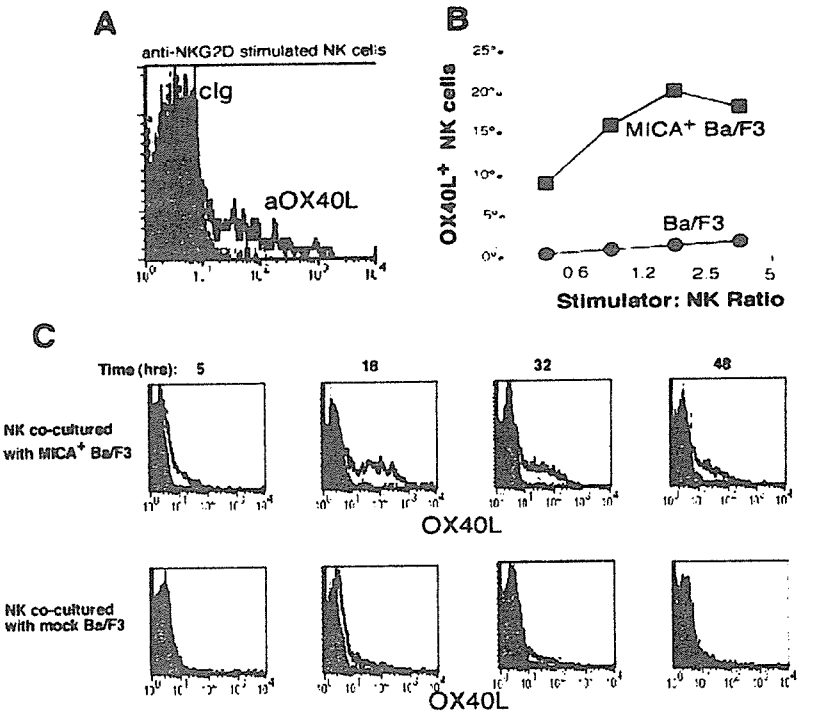

FIGURE 3. NKG2D stimulation induces OX40L on human polyclonal NK cells. *A*, Polyclonal human NK were activated with IL-2 for 72 h and stimulated with plate-bound anti-NKG2D mAb (thick line). Anti-CD56 mAb was used as a negative control of stimulation (dotted line). After 18 h of culture, cells were harvested and stained with FITC-conjugated anti-OX40L mAb (thick line, open histogram) or with cIg (filled histogram). A representative experiment of six is shown. *B*, IL-2-activated polyclonal NK cells were cultured with different numbers of mock Ba/F3 (●) or human MICA$^+$Ba/F3 (■) transfectants. After 18 h of coculture, NK cells were stained with anti-OX40L or control mAbs and the percentage of OX40L$^+$ NK cells is shown. A representative experiment of three is shown. *C*, Kinetics of OX40L induction on NK cells by coculture with NKG2D ligand-bearing cells. IL-2-activated polyclonal NK cells were cultured at a 1:2.5 stimulator:NK cell ratio with mock Ba/F3 (*lower panels*) or MICA$^+$Ba/F3 (*upper panels*) transfectants. Cells were harvested after 5, 18, 32, and 48 h of coculture, and stained anti-OX40L mAb (thick line, open histograms) and cIg (filled histograms). A representative experiment of three is shown.

restricted to either of these functionally distinct subsets defined by levels of CD56 and CD16 expression. In experiments combining both anti-NKG2D and anti-CD16 mAb stimulation (using optimal and saturating concentrations of both mAbs), the proportion of peripheral blood NK cells that expressed OX40L was equivalent to using optimal stimulation with anti-CD16 alone (data not shown).

NK cell costimulation of TCR-dependent CD4$^+$ T cell proliferation via OX40L-OX40 interactions

Our preliminary studies demonstrated that the OX40L$^+$ NKL leukemic cells were able to augment the proliferation of allogeneic human resting peripheral blood CD4$^+$ T cells stimulated with anti-CD3 mAb or PHA. The proliferation was partially, but substantially, inhibited by using a neutralizing anti-OX40L mAb (Fig. 1*B*). To address the potential interactions between NK cells CD4$^+$ T cells in a more physiological context, we performed additional experiments using autologous NK cells and CD4$^+$ T cells. We assayed proliferation induced not only by anti-CD3 mAb, but also by using autologous activated human NK cells (that express HLA-DR) to present SEB to autologous resting CD4$^+$ T cells. Because we had determined that anti-CD16 was more efficient than anti-NKG2D for inducing OX40L on peripheral blood NK cells, this system was chosen to evaluate the role of OX40L in the interactions between NK cells and autologous CD4$^+$ T cells. Highly purified, IL-2-preactivated peripheral blood NK cells were stimulated with anti-CD16 mAb, the NK cells were paraformaldehyde-fixed to prevent their proliferation or secretion of cytokines, and these cells were cocultured at varying ratios with highly purified resting autologous CD4$^+$ T cells in the presence of soluble anti-CD3 mAb. As shown in Fig. 4*A*, CD16-activated autologous NK cells efficiently costimulated anti-CD3-induced proliferation of CD4$^+$ T cells. This TCR-induced T cell proliferation was in part dependent upon OX40–OX40L interactions, because the proliferation was inhibited on average 60% (based on experiments using NK and T cells from seven different blood donors), in cultures containing the anti-OX40L specific neutralizing mAb 5A8. IL-2-activated NK cells that did not express OX40L were also able to costimulate the anti-CD3-induced proliferation of autologous CD4$^+$ T cells; however, this was always of a lower magnitude (approximately one third) than when the NK cells expressed OX40L as a consequence of prior stimulation via CD16 (Fig. 4*B*). An analysis of cytokines produced in these cultures revealed that the NK cell-costimulated T cells produced IFN-γ, but not IL-4 (Fig. 4*C*). Similar to the effects observed in the proliferation assays, anti-OX40L partially, but substantially, inhibited IFN-γ secretion induced by NK cell costimulation. In these experiments, fixed activated NK cells were used for costimulation to avoid the proliferation of the NK cells in response to IL-2, confirming that CD4$^+$ T cells were the responding population in the cultures, and to exclude that NK cell-derived cytokines were required for costimulation. We also established autologous NK:T cell cocultures with irradiated NK cells, and similar to fixed activated NK cells, irradiated activated NK also efficiently costimulated T cell proliferation in a OX40–OX40L dependent manner (data not shown).

Next, we investigated the role of OX40-OX40L interactions in autologous NK:T cell cocultures in response to a physiological TCR ligand, rather than anti-CD3 mAb. Bacterial superantigens bind with high affinity to MHC class II Ags on APCs and with TCR β-chains on the responding T cells. This results in the T cell activation responsible for toxic shock syndrome and food poisoning. Activated NK cells express MHC class II molecules (36, 37) and present SEB to T lymphocytes (37). Thus, anti-CD16-activated MHC class II-positive NK cells and autologous freshly isolated resting CD4$^+$ T cells were cultured in the presence of different concentrations of SEB. As shown in Fig. 5*A*, activated NK cells efficiently present SEB to autologous CD4$^+$ T cells, stimulating T cell proliferation. Furthermore, OX40-OX40L interactions were required for optimal T cell proliferation, as shown in Fig. 5*B* by the ability of anti-OX40L mAb to substantially inhibit SEB-induced T cell proliferation. Collectively, these data indicate that CD16-activated NK cells can efficiently costimulate anti-CD3 or SEB-induced proliferation of autologous CD4$^+$ T cells, and that OX40L-OX40 interactions are critically involved.

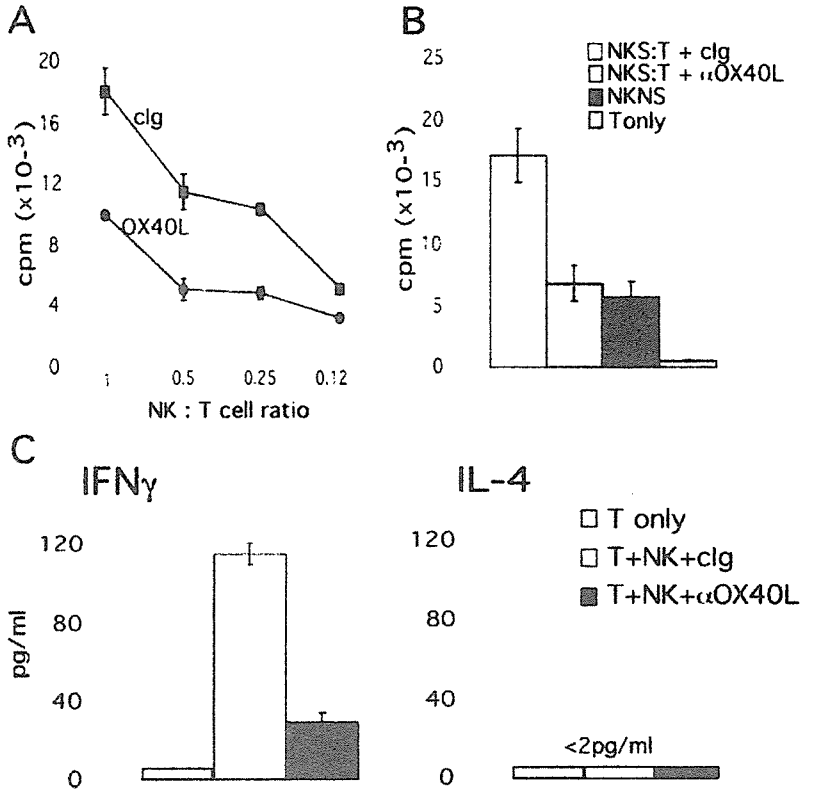

FIGURE 4. Anti-CD3 induced $CD4^+$ T cell proliferation and IFN-γ production costimulated by OX40L on autologous CD16-activated NK cells. *A*, IL-2-activated polyclonal NK cells were stimulated with plate-bound anti-CD16 mAb and fixed with 1% paraformaldehyde. Different numbers of anti-CD16-activated NK cells were plated with 1×10^5 autologous resting $CD4^+$ T cells in the presence of soluble anti-CD3 and cultured as described in Fig. 1*B*. Neutralizing anti-OX40L mAb or a cIg was added at day 0. A representative experiment of four is shown. Data are represented as the mean of cpm ± SD (triplicates). *B*, Cocultures of autologous activated NK cells and resting $CD4^+$ T cells at a ratio of 1:1 were established as described in Fig. 4*A*, using anti-CD16-stimulated NK cells (NKS) or cIg (anti-CD56 mAb)-treated NK cells (NKNS). Neutralizing anti-OX40L mAb or a cIg was added to the coculture of NKS and autologous $CD4^+$ T cells stimulated with anti-CD3, as indicated. Data are represented as the mean of cpm ± SE of seven independent experiments. *C*, Activated NK cell-resting $CD4^+$ T cell cocultures stimulated with anti-CD3 mAb were established as described in Fig. 4*A*. Neutralizing anti-OX40L mAb or a cIg was added to the cocultures, as indicated. Supernatants were collected after 72 h and tested for the presence of IFN-γ or IL-4. Data are represented as the mean ± SD (triplicates). A representative experiment of three is shown.

OX40L and B7 contribute to NK cell costimulation of $CD4^+$ T cell

We considered that the inability of anti-OX40L mAb to completely block $CD4^+$ T cell proliferation induced by activated NK cells may be due to the presence of CD86 (and perhaps CD80) on the activated NK cells (Fig. 2, *C* and *D*). Therefore, additional experiments were performed in which CD16-stimulated NK cells were cocultured with autologous $CD4^+$ T cells and anti-CD3 using a mixture of neutralizing mAbs against CD80 and CD86 (38) alone or in combination with anti-OX40L (Fig. 6). Interestingly, while mAbs against CD80 plus CD86 or OX40L individually partially inhibited NK cell-induced T cell proliferation, we observed that the combination of neutralizing mAbs against CD80, CD86, and OX40L completely blocked TCR-dependent $CD4^+$ T cell proliferation (results from two different blood donors are shown and are representative of five experiments). Collectively, these data show that CD16-stimulated NK cells efficiently costimulate TCR-dependent $CD4^+$ T cell proliferation through the expression of OX40L and B7-family members on the CD16-activated NK cells.

Discussion

Although it has been appreciated that NK cell production of IFN-γ and possibly other cytokines and chemokines can affect innate and adaptive immune responses, the potential role for direct cell-cell interactions between NK cells and T lymphocytes, in particular $CD4^+$ T cells, has not been explored. Roncarolo and colleagues (39) previously reported that human NK cell clones are able to stimulate autologous $CD4^+$ T cells, but the molecules involved in this process were not defined. Our unexpected finding that OX40L was up-regulated when NK cell receptors were stimulated on a transformed NK cell line prompted us to re-evaluate how activated NK cells are able to augment the TCR-dependent proliferation of resting autologous peripheral blood $CD4^+$ T cells. In this study, we provide evidence that activated human NK cells are able to help TCR-stimulated autologous $CD4^+$ T cells by a process that involves both OX40L and B7 costimulation.

Resting peripheral blood NK cells express neither OX40L nor B7, and different stimuli are required to induce these costimulatory molecules. Culture in IL-2 alone was sufficient to induce CD86, but not OX40L. By contrast, stimulation with IL-2 and activation through an NK receptor was required to induce OX40L. In addition to IL-2, IL-12 and IL-15 were also able to prime NK cells such that they up-regulated OX40L when subsequently stimulated via CD16. Because IL-12 and IL-15 are innate cytokines that may be more available at a site of inflammation or an ongoing immune response, these may represent the more physiologically relevant cytokines in vivo.

With respect to the NK receptors that induced OX40L, our first clues were derived from studies of the transformed NKL cell line. Although this cell constitutively expressed OX40L, it can be up-regulated by engaging either the DAP12-associated KIR2DS2 receptor that activates the Syk and ZAP70 tyrosine kinase pathways (40), or by stimulating the DAP10-associated NKG2D receptor that uses a PI3K-dependent activation pathway (33). We do not have Abs that can discriminate between the activating and inhibitory KIR; therefore, in studies of peripheral blood NK cells, we stimulated the NK cells with anti-CD16, which couples to the ITAM-bearing FcεRIγ and CD3ζ adapter proteins and activates Syk and ZAP70. When IL-2-preactivated peripheral blood NK cells were stimulated with either anti-CD16 or anti-NKG2D (or exposed to cells expressing the NKG2D ligand, MICA), OX40L was rapidly induced. Interestingly, only a subset comprising ~20% of the peripheral blood NK cells expressed OX40L after stimulating NKG2D, despite the fact that essentially all of the NK cells expressed NKG2D. Further studies are needed to determine why expression of OX40L was confined to a subset of the NKG2D-activated NK cells. By contrast, a much larger frequency of NK cells (typically 60% or more) expressed OX40L after CD16

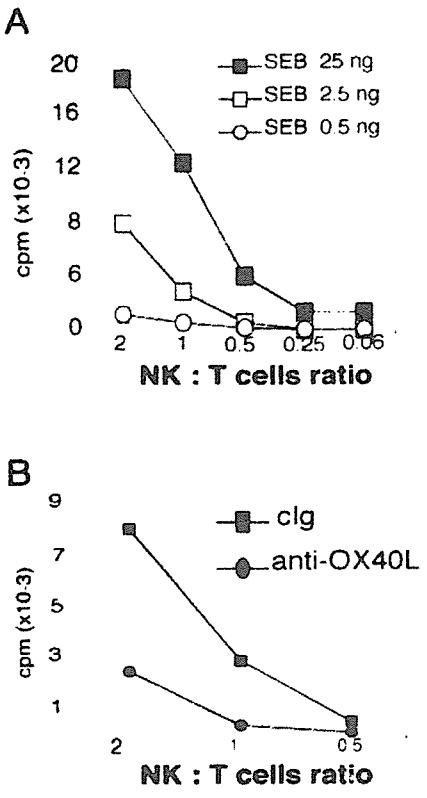

FIGURE 5. OX40L expressed on autologous NK receptor-activated NK cells is involved in SEB-induced proliferation of $CD4^+$ T cells. *A*, Anti-CD16-activated NK cells were prepared as described in Fig. 4*A*. Autologous resting $CD4^+$ T cells and activated NK cells were cocultured for 5 days in the presence of different concentrations of SEB, as indicated. Data are represented as the mean of cpm ± SD (triplicates). A representative experiment of two is shown. *B*, Autologous resting $CD4^+$ T cells and anti-CD16-activated NK cells at the indicated ratios were cocultured in the presence of 2.5 ng/ml SEB for 5 days. Neutralizing anti-OX40L mAb or cIg was added at day 0. Data are represented as the mean of cpm ± SD (triplicates). A representative experiment of three is shown.

activation. Many of the NK receptors, e.g., NKp30, NKp44, NKp46, CD16, and the activating KIR (41), use ITAM-based adapter proteins to activate the Syk/ZAP70 tyrosine kinases. Therefore, we suspect that OX40L may be induced when any of these diverse receptors are engaged because they use a common downstream signaling pathway. Together with the ability of IL-2, IL-12, or IL-15 to render the NK cells permissive for NK receptor induction of OX40L, our findings indicate that OX40L may be available in many different physiological situations for potential interactions with T cells bearing OX40.

Where might activated NK cells and $CD4^+$ T cells interact? This interaction might happen in peripheral tissues such as the liver in which both NK cells and T cells are resident (42) and accumulate following virus infection (43). Furthermore, a recent report has revealed that NK cells are relatively abundant in the human secondary lymphoid organs (44), and importantly, immunohistochemistry studies have detected NK cells in the parafollicular T cell areas of human lymph nodes (24), providing another possible location in which NK:T cell interactions might occur during an immune response. During a viral or bacterial infection, NK cells in the lymph nodes may be exposed to an environment containing IL-2, IL-12, or IL-15, and potential NKG2D ligands or immune complexes (that engage CD16), thereby providing the stimuli needed for induction of OX40L and allowing them to interact with activated $CD4^+$ T cell-expressing OX40.

It should be appreciated that activated human NK cells express high levels of MHC class II (36, 37), which provides them the potential to present Ag to human $CD4^+$ T cells. Indeed, in these studies, we have shown that activated NK cells have the capability to directly stimulate $CD4^+$ T cell proliferation by presenting SEB to $CD4^+$ T cells. Therefore, activated human NK cells possess not only the required costimulatory molecules (e.g., OX40L and B7) for potential interaction with activated $CD4^+$ cells, but they also, in theory, have the capacity of present Ags via MHC class II. Collectively, our in vitro experiments provide compelling evidence that human NK cells and autologous $CD4^+$ cells can interact and that OX40L is an important participant in this process. It is difficult to provide formal proof of this interaction in vivo in humans. Unfortunately, because activated mouse NK cells (unlike human NK cells) do not express MHC class II, mice do not provide a relevant or appropriate model to examine MHC class II TCR-dependent $CD4^+$ cell interactions with NK cells. Although dendritic cells are considered the most potent APCs, the fact that activated NK cells express MHC class II, CD86, and OX40L strongly suggests the possibility that they may also communicate directly with $CD4^+$ cells. Otherwise, for what purpose would NK receptor-activated human NK cells express MHC class II, CD86, and OX40L?

Our findings demonstrate that human NK cell costimulation of TCR-induced $CD4^+$ T proliferation depends in a large part on OX40–OX40L interactions. Studies conducted using OX40-deficient mice have shown that OX40-deficient $CD4^+$ T cells initially become activated to secrete IL-2 (albeit at slightly lower levels than wild-type mice), but they are unable to sustain proliferation (45). Other studies performed on $OX40^{-/-}$ mice reported that the impaired in vitro proliferative response to anti-CD3 stimulation

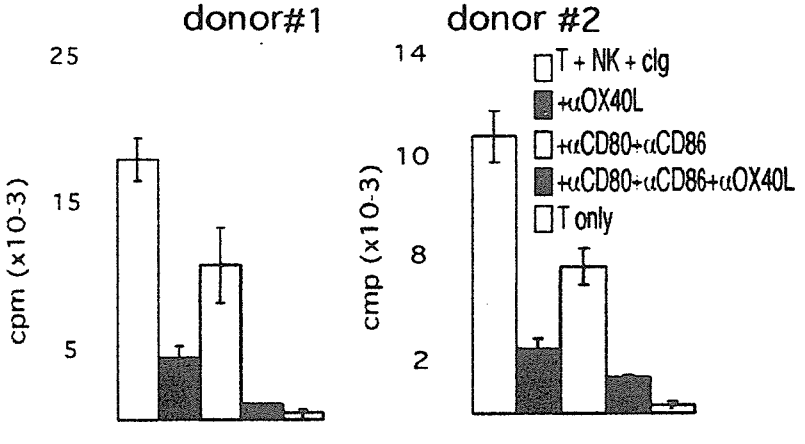

FIGURE 6. NK cell costimulation of TCR-dependent $CD4^+$ T cell proliferation involves B7 family members. Cocultures of anti-CD16-stimulated autologous NK and $CD4^+$ T cells at a ratio of 1:1 were established and stimulated with anti-CD3 as described in Fig. 4*A*. Neutralizing mAbs against CD80, CD86, and/or OX40L or cIg, as indicated, were added on day 0 at 5 μg/ml. Data are represented as the mean ± SD (triplicates). Two representative experiments of five are shown.

could not be corrected by the addition of exogenous rIL-2 (46). Most significantly, it has been shown that OX40 is a major regulator of anti-apoptotic proteins, such as Bcl-xL and Bcl-2 (45), and strongly promotes the survival of Ag-activated primary $CD4^+$ T cells (11). Similarly, the contribution of OX40-OX40L interactions to T cell proliferation that we have observed may favor T cell survival by the induction of Bcl-xL and Bcl-2, although this awaits further evaluation.

Previous studies reported that OX40L expressed on mouse B cells induce a Th2-type response, leading to the expansion of IL-4-producing mouse T effector cells and inhibiting IFN-γ expression (47, 48). In humans, a role for OX40L in the development of Th2 effector cells has also been reported (49). However, other studies do not support a differential role for OX40L in inducing Th1 vs Th2 differentiation (11, 13, 50, 51). suggesting that it only enhances the pre-existing response. In our studies using activated human NK cells to costimulate autologous $CD4^+$ T cells, we observed the production of IFN-γ, but not IL-4 secretion, by the TCR-activated T cells. These findings suggest that activated, mature human NK cells may preferentially promote T cell IFN-γ production.

We believe that the induction of OX40L on NK cells by NKG2D ligand-expressing cells might have important implications in the context of tumor surveillance and infectious diseases. It has been shown that the NKG2D ligand MICA is up-regulated on several human tumor cells and, interestingly, soluble MICA has been found in the serum of patients affected by different progressive tumors (52). In addition, several studies have reported that MICA is induced on cells infected with *Mycobacteria tuberculosis* (18), *Escherichia coli* (19), or cytomegalovirus (17). Thus, initial interactions between NK cells and NKG2D ligand-bearing cells or soluble NKG2D ligands may trigger killing and cytokine production and in the presence of IL-2, IL-15, or IL-12 may induce expression of OX40L on the NK cells. Subsequent interactions between $OX40L^+$ NK cells and $OX40^+$ T cells may amplify and sustain an adaptive ongoing immune response. At least under the experimental conditions used, we observed the induction of OX40L only on a subset of activated human peripheral blood NK cells. Further studies are necessary to resolve why some NK cells, but not others, expressed OX40L upon NKG2D stimulation, because all NK cells express NKG2D on the cell surface.

The OX40-OX40L interaction has been shown to induce bidirectional signals. For example, OX40L stimulation by OX40 transduces a signal in dendritic cells, which results in enhanced TNF-α and IL-1β production (2). Similarly, triggering of OX40L expressed on activated B cells results in B cell proliferation and Ig secretion (53). Finally, engagement of OX40L on vascular endothelial cells leads to the induction of c-*fos* and c-*jun* mRNA expression and the production of the chemokine RANTES (54, 55). Thus, while our present studies have focused on the potential role of OX40L on NK cell interactions with $CD4^+$ T cells, it will also be of interest to examine whether engagement of OX40L on NK cells might regulate their effector functions.

Acknowledgments

We thank Dr. Nigel Killeen and Dr. Cristina Cerboni for helpful discussion.

References

1. Croft, M. 2003. Co-stimulatory members of the TNFR family: keys to effective T-cell immunity? *Nat. Rev. Immunol. 3:609.*
2. Ohshima, Y., Y. Tanaka, H. Tozawa, Y. Takahashi, C. Maliszewski, and G. Delespesse. 1997. Expression and function of OX40 ligand on human dendritic cells. *J. Immunol. 159:3838.*
3. Stuber, E., and W. Strober. 1996. The T cell-B cell interaction via OX40-OX40L is necessary for the T cell dependent humoral immune response. *J. Exp. Med. 183:979.*
4. Imura, A., T. Hori, T. Imada, T. Ishikawa, Y. Tanaka, M. Maeda, S. Imamura, and T. Uchiyama. 1996. The human OX40/gp34 system directly mediates adhesion of activated T cells to vascular endothelial cells. *J. Exp. Med. 183:2185.*
5. Kim, M. Y., F. Gaspal, H. Wiggett, F. McConnell, A. Gulbranson-Judge, R. C., L. Walker, M. Goodall, and P. Lane. 2003. $CD4^+CD3^-$ accessory cells costimulate primed CD4 T cells through OX40 and CD30 at sites where T cells collaborate with B cells. *Immunity 18:643.*
6. Weinberg, A. D. 2002. OX40: targeted immunotherapy — implications for tempering autoimmunity and enhancing vaccines. *Trends Immunol. 23:102.*
7. Brugnoni, D., A. Bettinardi, F. Malacarne, P. Airo, and R. Cattaneo. 1998. CD134/OX40 expression by synovial fluid $CD4^+$ T lymphocytes in chronic synovitis. *Br. J. Rheumatol. 37:584.*
8. Tittle, T. V., A. D. Weinberg, C. N. Steinkeler, and R. T. Maziarz. 1997. Expression of the T-cell activation antigen, OX-40, identifies alloreactive T cells in acute graft-versus-host disease. *Blood 89:4652.*
9. Vetto, J. T., S. Lum, A. Morris, M. Sicotte, J. Davis, M. Lemon, and A. Weinberg. 1997. Presence of the T-cell activation marker OX-40 on tumor infiltrating lymphocytes and draining lymph node cells from patients with melanoma and head and neck cancers. *Am. J. Surg. 174:258.*
10. Gramaglia, I., A. D. Weinberg, M. Lemon, and M. Croft. 1998. Ox-40 ligand: a potent costimulatory molecule for sustaining primary CD4 T cell response. *J. Immunol. 161:6510.*
11. Gramaglia, I., A. Jember, S. D. Pipping, A. D. Weinberg, N. Killeen, and M. Croft. 2000. The OX40 costimulatory receptor determines the development of CD4 memory by regulating primary clonal expansion. *J. Immunol. 165:3043.*
12. Weinberg, A. D., M. M. Rivera, R. Prell, A. Morris, T. Ramstad, J. T. Veto, W. J. Urba, G. Alvord, C. Bunce, and J. Shields. 2000. Engagement of the OX40 receptor in vivo enhances antitumour immunity. *J. Immunol. 164:2160.*
13. Kopf, M., C. Ruedi, N. Schimitz, A. Gallimore, K. Lefrang, B. Ecabert, B. Odermatt, and M. F. Bachmann. 1999. Ox40–deficient mice are defective in Th cell proliferation but are competent in generating B cell and CTL responses after virus infection. *Immunity 11:699.*
14. Lanier, L. L. 2001. On guard: activating NK receptors. *Nat. Rev. Immunol. 2:3.*
15. Bauer, S., V. Groh, J. Wu, A. Steinle, J. H. Phillips, L. L. Lanier, and T. Spies. 1999. Activation of NK cells and T cells by NKG2D, a receptor for stress-inducible MICA. *Science 285:727.*
16. Cosman, D., J. Mullberg, C. L. Sutherland, W. Chin, R. Armitage, W. Fanslow, M. Kubin, and N. J. Chalupny. 2001. ULBPs, novel MHC class I-related molecules, bind to CMV glycoprotein UL16 and stimulate NK cytotoxicity through the NKG2D receptor. *Immunity 14:123.*
17. Groh, V., R. Rhinehart, J. Randolf-Habecker, M. S. Topp, S. R. Riddell, and T. Spies. 2001. Costimulation of CD8 $\alpha\beta$ T cells by NKG2D via engagement by MIC induced on virus-infected cells. *Nat. Immunol. 2:255.*
18. Das, H., V. Groh, C. Kuij, M. Sugita, C. T. Morita, T. Spies, and J. F. Bukowski. 2001. MICA engagement by human Vg2Vd2 T cells enhances their antigen-dependent effector function. *Immunity 15:83.*
19. Tieng, V., D. Bougu'enec, L. Du Merle, P. Bertheau, P. Desreumaux, A. Janin, D. Charron, and A. Toubert. 2002. Binding of *Escherichia coli* adhesin AfaE to CD55 triggers cell-surface expression of the MHC class I-related molecule MICA. *Proc. Natl. Acad. Sci. USA 99:2977.*
20. Groh, V., R. Rhinehart, H. Secrist, S. Bauer, A. Greght, and T. Spies. 1999. Broad tumour-associated expression and recognition by tumour derived $\gamma\delta$ T cells of MICA and MICB. *Proc. Natl. Acad. Sci. USA 96:6879.*
21. Groh, V., S. Bahram, S. Bauer, A. Herman, M. Beauchamp, and T. Spies. 1996. Cell stress–regulated human major histocompatibility complex class I gene expressed in gastrointestinal epithelium. *Proc. Natl. Acad. Sci. USA 93:12445.*
22. Biron, C. A., K. B. Nguyen, G. C. Pien, L. P. Cousens, and T. P. Salazar-Mather. 1999. Natural killer cells in antiviral defence: function and regulation by innate cytokines. *Annu. Rev. Immunol. 17:189.*
23. Moretta, A. 2002. Natural Killer cells and dendritic cells: rendezvous in abused tissues. *Nat. Rev. Immunol. 2:957.*
24. Fehniger, T. A., M. A. Cooper, G. J. Nuovo, M. Cella, F. Facchetti, M. Colonna, and M. Caligiuri. 2003. $CD56^{bright}$ natural killer cells are present in human lymph nodes and are activated by T cell-derived IL-2: a potential new link between adaptive and innate immunity. *Blood 101:3052.*
25. Robertson, M. J., K. J. Cochran, C. Cameron, J. M. Le, R. Tantravahi, and J. Ritz. 1996. Characterization of a cell line, NKL, derived from an aggressive human natural killer cell leukemia. *Exp. Hematol. 24:406.*
26. Wu, J., H. Cherwinski, T. Spies, J. H. Phillips, and L. L. Lanier. 2000. DAP10 and DAP12 form distinct, but functionally cooperative, receptor complexes in natural killer cells. *J. Exp. Med. 192:1059.*
27. Kinsella, T. M., and G. P. Nolan. 1996. Episomal vectors rapidly and stably produce high-titer recombinant retrovirus. *Hum. Gene Ther. 7:1405.*
28. Onishi, M., S. Kinoshita, Y. Morikawa, A. Shibuya, J. Phillips, L. L. Lanier, D. M. Gorman, G. P. Nolan, A. Miyajima, and T. Kitamura. 1996. Applications of retrovirus-mediated expression cloning. *Exp. Hematol. 24:324.*
29. Zingoni, A., G. Palmieri, S. Morrone, M. Carretero, M. Lopez-Botet, M. Piccoli, L. Frati, and A. Santoni. 2000. CD69-triggered ERK activation and functions are negatively regulated by CD94/NKG2-A inhibitory receptor. *Eur. J. Immunol. 30:644.*
30. De Risi, J. L., V. R. Iyer, and P. O. Brown. 1997. Exploring the metabolic and genetic control of gene expression on a genomic scale. *Science 278:680.*
31. Bandman, O., R. T. Coleman, J. F. Loring, J. J. Seilhamer, and B. G. Cocks. 2002. Complexity of inflammatory responses in endothelial cells and vascular

smooth muscle cells determined by microarray analysis. *Ann. NY Acad. Sci. 975:77.*
32. Yue, H., P. S. Eastman, B. B. Wang, J. Minor, M. H. Doctolero, R. L. Nuttall, R. Stack, J. W. Becker, J. R. Montgomery, M. Vainer, and R. Johnston. 2001. An evaluation of the performance of cDNA microarrays for detecting changes in global mRNA expression. *Nucleic Acids Res. 29:41.*
33. Wu, J., Y. Song, A. B. Bakker, S. Bauer, T. Spies, L. L. Lanier, and J. H. Phillips. 1999. An activating immunoreceptor complex formed by NKG2D and DAP10. *Science 285:730.*
34. Billadeau, D. D., J. L. Upshaw, R. A. Schoon, C. J. Dick, and P. J. Leibson. 2003. NKG2D-DAP10 triggers human NK cell-mediated killing via a Syk-independent regulatory pathway. *Nat. Immunol. 4:557.*
35. Kashii, Y., R. Giorda, R. B. Herberman, T. L. Whiteside, and N. L. Vujanovic. 1999. Constitutive expression and role of TNF family ligands in apoptotic killing of tumor cells by human NK cells. *J. Immunol. 163:5358.*
36. Phillips, J. H., A. M. Le, and L. L. Lanier. 1984. Natural killer cells activated in a human mixed lymphocyte response culture identified by expression of Leu-11 and class II histocompatibility antigens. *J. Exp. Med. 159:993.*
37. D'Orazio, J. A., and J. Stein-Streilein. 1996. Human natural killer cells present staphylococcal enterotoxin B (SEB) to T lymphocytes. *Clin. Exp. Immunol. 104:366.*
38. Lanier, L. L., S. O'Fallon, C. Somoza, J. H. Phillips, P. S. Linsley, K. Okumura, D. Ito, and M. Azuma. 1995. CD80 (B7) and CD86 (B70) provide similar costimulatory signals for T cell proliferation, cytokine production, and generation of CTL. *J. Immunol. 154:97.*
39. Roncarolo, M. G., M. Bigler, J. B. Haanen, H. Yssel, R. Bacchetta, J. E. de Vries, and H. Spits. 1991. Natural killer cell clones can efficiently process and present protein antigens. *J. Immunol. 147:781.*
40. Lanier, L. L., B. C. Corliss, J. Wu, C. Leong, and J. H. Phillips. 1998. Immunoreceptor DAP12 bearing a tyrosine-based activation motif is involved in activating NK cells. *Nature 391:703.*
41. Moretta, A., C. Bottino, M. Vitale, D. Pende, C. Cantoni, M. C. Mingari, R. Biassoni, and L. Moretta. 2001. Activating receptors and coreceptors involved in human natural killer cell-mediated cytolysis. *Annu. Rev. Immunol. 19:197.*
42. Crispe, I. 2003. Hepatic T cells and liver tolerance. *Nat. Rev. Immunol. 3:51.*
43. Salazar-Mather, T. P., T. A. Hamilton, and C. A. Biron. 2000. A chemokine-to-cytokine-to-chemokine cascade critical in antiviral defense. *J. Clin. Invest. 105:985.*
44. Ferlazzo, G., D. Thomas, S. L. Lin, K. Goodman, B. Morandi, W. A. Muller, A. Moretta, and C. Munz. 2004. The abundant NK cells in human secondary lymphoid tissues requires activation to express killer cell Ig-like receptors and become cytolytic. *J. Immunol. 172:1455.*
45. Rogers, P. R., J. Song, I. Gramaglia, N. Killeen, and M. Croft. 2001. OX40 promotes Bcl-xL and Bcl-2 expression and is essential for long term survival of CD4 T cells. *Immunity 15:445.*
46. Pipping, S. D., C. Pena-Rossi, J. Long, W. R. Godfrey, D. J. Fowell, S. L. Reiner, M. L. Birkeland, R. M. Locksley, A. N. Barclay, and N. Killeen. 1999. Robust B cell immunity but impaired T cell proliferation in the absence of CD134 (OX40). *J. Immunol. 163:6520.*
47. Linton, P.-J., B. Bautista, E. Biederman, E. S. Bradley, J. Harbertson, R. M. Kondrack, R. C. Patrick, and L. Bradley. 2003. Costimulation via OX40L expressed by B cells is sufficient to determine the extent of primary CD4 cell expansion and Th2 cytokine secretion in vivo. *J. Exp. Med. 197:875.*
48. Flynn, S., K.-M. Toellner, C. Raykundalia, M. Goodall, and P. Lane. 1998. CD4T cell cytokine differentiation: the B cell activation molecule, OX40L, instructs CD4T cells to express interleukin 4 and upregulates expression of the chemokine receptor, Blr-1. *J. Exp. Med. 188:297.*
49. Ohshima, Y., L.-P. Yang, T. Uchiyama, Y. Tanaka, P. Baum, M. Sergerie, P. Hermann, and G. Delespesse. 1998. Ox40 costimulation enhances interleukin-4 (IL-4) expression at priming and promotes the differentiation of naïve human $CD4^+$ T cells into high Il-4-producing effectors. *Blood 92:3338.*
50. De Smedt, T., J. Smith, P. Baum, W. Fanslow, E. Butz, and C. Maliszewski. 2002. Ox40 costimulation enhances the development of T cell responses induced by dendritic cells in vivo. *J. Immunol. 168:661.*
51. Chen, A. I., J. McAdam, J. E. Buhlmann, S. Scott, M. L. Lupher, E. A. Greenfield, P. R. Baum, W. C. Fanslow, D. M. Calderhead, G. J. Freeman, and A. H. Sharpe. 1999. OX40-ligand has a critical costimulatory role in dendritic cell:T cell interactions. *Immunity 11:689.*
52. Groh, V., J. Wu, C. See, and T. Spies. 2002. Tumour-derived soluble MIC ligands impair expression of NKG2D and T-cell activation. *Nature 419:734.*
53. Morimoto, S., Y. Kanno, Y. Tanaka, Y. Tokano, S. Hashimoto, S. Jacquot, C. Morimoto, S. F. Schlossman, H. Yagita, K. Okumura, and T. Kobata. 2000. CD134L engagement enhances human B cell Ig production: CD154/CD40, CD70/CD27, and CD134/CD134L interactions coordinately regulate T cell-dependent B cell responses. *J. Immunol. 164:4097.*
54. Matsumura, Y., T. Hori, S. Kawamata, A. Imura, and T. Uchiyama. 1999. Intracellular signaling of gp34, the OX40L: induction of c-*jun* and c-*fos* mRNA expression through gp34 upon binding of its receptor, OX40. *J. Immunol. 163:3007.*
55. Kotani, A., T. Hori, Y. Matsumura, and T. Uchiyama. 2002. Signaling of gp34 (OX40 ligand) induces vascular endothelial cells to produce a CC chemokine RANTES/CCL5. *Immunol. Lett. 84:1.*

ARTICLE

doi:10.1016/j.ymthe.2004.07.029

Competitive Repopulation Assay of Two Gene-Marked Cord Blood Units in NOD/SCID/γc^{null} Mice

Takashi Yahata,[1,2] Kiyoshi Ando,[1,2,*] Hiroko Miyatake,[1] Tomoko Uno,[1] Tadayuki Sato,[1] Mamoru Ito,[3] Shunichi Kato,[1,4] and Tomomitsu Hotta[1,2]

[1]*Division of Hematopoiesis, Research Center for Regenerative Medicine,* [2]*Department of Hematology, and* [4]*Department of Cell Transplantation & Regenerative Medicine, Tokai University School of Medicine, Isehara, Kanagawa 259-1193, Japan*

[3]*Central Institute for Experimental Animals, Kawasaki, Kanagawa 216-0001, Japan*

[*]*To whom correspondence and reprint requests should be addressed at the Department of Hematology, Tokai University School of Medicine Bohseidai, Isehara, Kanagawa 259-1193, Japan. Fax: +81 463 92 4511. E-mail: andok@keyaki.cc.u-tokai.ac.jp.*

Available online 2 September 2004

In multiunit cord blood transplantation, hematopoietic stem cells from each unrelated cord blood (UCB) unit competitively reconstitute the hematopoietic system in a recipient. To evaluate the fate of the progeny of each UCB unit and to determine the effects of graft-versus-graft reaction, we established a novel competitive repopulation assay using NOD/SCID/γc^{null} mice in which human T lymphocytes develop from $CD34^+$ cells. $CD34^+$ cells from each UCB unit were labeled with recombinant lentivirus vectors carrying genes encoding either enhanced green fluorescent protein (EGFP) or enhanced yellow fluorescent protein (EYFP). Hematopoietic chimerism composed of both $EGFP^+$ and $EYFP^+$ cells was stably maintained up to 6 months after transplantation with purified $CD34^+$ cells; the ratio of $EGFP^+$ to $EYFP^+$ cells in peripheral blood and bone marrow posttransplantation was equivalent to the ratio of these cells at transplantation. However, when mononuclear cells from two UCB units were cotransplanted with $CD34^+$ cells, engraftment was highly competitive, with cells from only one or the other of the two UCB units surviving. Further subfractionations of mononuclear cells indicate that the skewed chimerism that is often observed in clinical multiunit cord blood transplantation may be mediated by the cooperation of both $CD4^+$ and $CD8^+$ T cells. The assay established here will be a useful tool for analyzing hematopoietic reconstitution in clinical multiunit cord blood transplantation.

Key Words: gene marking, lentivirus, hematopoietic stem cell, SCID mouse-repopulating cell assay, multiunit cord blood transplantation, NOG mouse, competitive repopulation assay

INTRODUCTION

Cord blood (CB) is a potentially rich alternate source of hematopoietic stem cells (HSCs) and progenitors for clinical allogeneic transplantation [1,2]. Despite some promising outcomes with unrelated cord blood transplantation (UCBT) in pediatric recipients, the low cell content of the graft relative to recipient size may adversely affect both the time to hematopoietic recovery and survival [3–6]. Therefore, the major limitation to the widespread use of unrelated CB (UCB) as a source of HSC for transplantation, particularly in adults, is the low yield of stem cells. To overcome this, several centers have initiated multiunit UCBT (m-UCBT) in which two or more units of closely HLA-matched UCB are transplanted [7–9].

In clinical m-UCBT, HSCs from multiple UCB units competitively reconstitute the hematopoietic and immune systems, raising the possibility of a graft-versus-graft reaction or of multiple graft-versus-host reactions. Although an *in vivo* competitive repopulation assay has been widely used in mice [10–12], dogs [13], and nonhuman primates [14,15] to evaluate the potency of HSCs for hematopoietic reconstitution, there is currently no practical assay system for competitive repopulation by human HSCs, which might help to predict the results of graft-versus-graft reactions and immune reconstitution by multiple UCBs.

Xenogeneic transplantation models, in particular the severe combined immunodeficient (SCID) mouse-repopulating cell assay, have been used to evaluate *in vivo* human HSC activity, such as self-renewal and multilineage differentiation [16–19]. The nonobese diabetic (NOD)/SCID mice and related strains have

1525-0016/$30.00